



Ice-margin and meltwater dynamics during the mid-Holocene in the Kangerlussuaq area of west Greenland

Carrivick, Jonathan L.; Yde, Jacob; Russell, Andrew J.; Quincey, Duncan J.; Ingeman-Nielsen, Thomas; Mallalieu, Joseph

Published in:
Boreas

Link to article, DOI:
[10.1111/bor.12199](https://doi.org/10.1111/bor.12199)

Publication date:
2017

Document Version
Peer reviewed version

[Link back to DTU Orbit](#)

Citation (APA):
Carrivick, J. L., Yde, J., Russell, A. J., Quincey, D. J., Ingeman-Nielsen, T., & Mallalieu, J. (2017). Ice-margin and meltwater dynamics during the mid-Holocene in the Kangerlussuaq area of west Greenland. *Boreas*, 46(3), 369-387. <https://doi.org/10.1111/bor.12199>

General rights

Copyright and moral rights for the publications made accessible in the public portal are retained by the authors and/or other copyright owners and it is a condition of accessing publications that users recognise and abide by the legal requirements associated with these rights.

- Users may download and print one copy of any publication from the public portal for the purpose of private study or research.
- You may not further distribute the material or use it for any profit-making activity or commercial gain
- You may freely distribute the URL identifying the publication in the public portal

If you believe that this document breaches copyright please contact us providing details, and we will remove access to the work immediately and investigate your claim.

Ice margin and meltwater dynamics during the mid-Holocene in the Kangerlussuaq area of west Greenland

JONATHAN L. CARRIVICK, JACOB YDE, ANDREW J. RUSSELL, DUNCAN J. QUINCEY,
THOMAS INGEMAN-NIELSEN AND JOSEPH MALLALIEU

Carrivick, J.L., Yde, J., Russell, A.J., Quincey, D.J., Ingeman-Nielsen, T., and Mallalieu, J.: Ice margin and meltwater dynamics during the mid-Holocene in the Kangerlussuaq area of west Greenland. *Boreas* doi xxxxxx

Land-terminating parts of the west Greenland ice sheet have exhibited highly dynamic meltwater regimes over the last few decades including episodes of extremely intense runoff driven by ice surface ablation, ponding of meltwater in an increasing number and size of lakes, and sudden outburst floods, or 'jökulhlaups', from these lakes. However, whether this meltwater runoff regime is unusual in a Holocene context has not been questioned. This study assembled high-resolution topographic data, geological and landcover data, and produced a glacial geomorphological map covering ~1200 km². Digital analysis of the landforms reveals a mid-Holocene land-terminating ice margin that was predominantly cold-based. This ice margin underwent sustained active retreat but with multiple minor advances. During ~1000 years meltwater runoff became impounded within numerous and extensive proglacial lakes and there were temporary connections between some of these lakes via spillways. The ice-dams of some of these lakes had several quasi-stable thicknesses. Meltwater was apparently predominantly from supraglacial sources although some distributary palaeochannel networks and some larger bedrock palaeochannels most likely relate to mid-Holocene subglacial hydrology. In comparison to the geomorphological record at other northern Hemisphere ice sheet margins the depositional landforms in this study area are few in number and variety and small in scale, most likely due to a restricted sediment supply. They include perched fans and deltas and perched braidplain terraces. Overall, meltwater sourcing, routing and the proglacial runoff regime during the mid-Holocene in this land-terminating part of the ice sheet was spatio-temporally variable, but in a manner very similar to that of the present day.

Jonathan L. Carrivick (j.l.carrivick@leeds.ac.uk), Duncan J. Quincey and Joseph Mallalieu, School of Geography and water@leeds, University of Leeds, Woodhouse Lane, Leeds, LS2 9JT, UK; Jacob Yde, Sogn og Fjordane University College, NO-6851 Sogndal, Norway; Andrew J. Russell, School of Geography, Politics & Sociology, Newcastle University, Newcastle-upon-Tyne, NE1 7RU, UK; Thomas Ingeman-Nielsen, Arctic Technology Centre, Technical University of Denmark, Kemitovet, Building 204, DK-2800 Kgs. Lyngby, Denmark; received xx/xx/xx, accepted xx/xx/2016

39 Changes in terminus position, mass and dynamics of land-terminating outlet glaciers in
40 west Greenland have major implications for ice sheet stability and via meltwater fluxes
41 for global sea level rise. A key to understanding the driving mechanisms of dynamic
42 changes has been separating short-term variability from longer-term trends, in air
43 temperatures, ice sheet surface melt, and outlet glacier velocity, for example. Specifically,
44 analyses of remotely-sensed images of the ice surface have enabled surface meltwater
45 generation (e.g. Harper *et al.* 2012), temporary storage in supraglacial lakes (e.g.
46 Fitzpatrick *et al.* 2014), and the implications for subglacial meltwater dynamics (e.g.
47 Bartholomew *et al.* 2012) and glacier velocity (e.g. van de Wal *et al.* 2015), to be
48 interpreted over the last decade. Mernild *et al.* (2012) have compared modelled
49 variability in meltwater runoff to that measured, and Carrivick & Quincey (2014) have
50 analysed variability in the number and size of ice marginal lakes along the entire western
51 margin. However, even the most long-term of these studies is limited to the satellite era
52 and to the duration of field campaigns, i.e. over the last ~ 45 years at most and usually
53 concentrated in the last decade. There is therefore a need to utilise longer-term datasets,
54 such as glacial geomorphology, to place modern observations of land-terminating ice
55 margin position fluctuations and the regime(s) of meltwater from these in the context of
56 longer-term (Holocene) ice sheet margin character and behaviour.

57

58 Previous research on Holocene glacial geomorphology associated with the land-
59 terminating margins of the ice sheet in west Greenland has been motivated to establish a
60 geochronology, i.e. identifying and absolute dating of major (Last Glacial Maximum and
61 Holocene) moraines, and improving the resolution/confidence of these dates. Major
62 efforts have concentrated on evidence pertaining to the early Holocene in the
63 Qeqertarsuaq (Disko Island) – Disko Bugt area (e.g. Donner & Jungner 1975; Ingólfsson
64 *et al.* 1990; Humlum *et al.* 1995; Long & Roberts 2002; Lloyd *et al.* 2005, Long *et al.*
65 2006; Young *et al.* 2013), or on terrestrial evidence pertaining to the middle Holocene in
66 the Sisimiut-Kangerlussuq area (e.g. Ten Brink & Weidick 1974; Ten Brink 1975; van
67 Tatenhove *et al.* 1996; Levy *et al.* 2012). In recent years the use of cosmogenic surface
68 exposure dating has added additional information to the chronology of the Late-
69 Wisconsin and Holocene deglaciation history (e.g. Rinterknecht *et al.* 2009; Roberts *et al.*
70 2010). Overall, whilst major moraine systems spanning ~ 120 km of landscape have been
71 mapped in west Greenland (Ten Brink 1975), there is a paucity of ‘high-resolution’ glacial

72 geomorphological mapping and thus of complementary detailed information on the
73 former ice areal extent, thickness, flow patterns and behaviour. By far the most notable
74 exception is the seminal work of Ten Brink (1975) who made detailed investigations of
75 the major moraine systems, glacial geomorphology and Holocene history of the
76 Sukkertoppen – Kangerlussuaq – Ørkendalen (Qinnguata Kuussua) area but who was
77 limited by glacial deposits that were < 50 m in local relief (Ten Brink 1975) and, in general
78 ‘a thin drift with little topography’ (Ten Brink, 1975). Warren & Hulton (1990) made a
79 glacial geomorphology investigation south of Ilulissat (Jakobshavn) and interpreted a
80 topographic control (rather than climate) on still-stands of a retreating tidewater outlet
81 glacier.

82

83 The aim of this study is therefore to critically analyse the landform record of ice
84 margin and meltwater activity during the mid-Holocene in west Greenland. This is
85 achieved via construction of a high-resolution glacial geomorphological map, taking
86 advantage of digital terrain analysis where possible, in combination with geological data,
87 landcover data and field observations. We focus on the Kangerlussuaq area because of its
88 accessibility and its prominence in ongoing research into the nearby glaciers, rivers,
89 geology, soils and vegetation.

90

91 **Study site**

92 The Kangerlussuaq area (Fig. 1) has an arid, continental low-arctic climate (Mernild *et al.*
93 2015). The bedrock in the area is predominantly of Archaean ortho-gneisses that were
94 reworked under high grade metamorphism in the palaeo-proterozoic (Van Gool *et al.*
95 2002). The bedrock mainly has a dip of 70° east and there are several major faults and
96 joints extending through the area (Aaltonen *et al.* 2010). The large-scale topography (Fig.
97 1), which is primarily controlled by these faults and joints, has been further exaggerated
98 by glacial erosion that formed U-shaped valleys and produced areal scouring (Sugden
99 1974), and subsequently post-glacial faulting that provides a lineation predominantly in
100 the east-west direction (Aaltonen *et al.* 2010). The meso-scale topography is typical of
101 area scouring by subglacial erosion of crystalline bedrock and includes dome-like
102 summits, rounded ridges, smoothed floors of incised cols, and streamlined ‘stoss and lee’
103 bedrock hummocks (Sugden 1974; Ten Brink 1975). Valley fill deposits at the fjord heads

104 include major terraces that are composed of both glacial and marine sediments (e.g.
105 Storms *et al.* 2012).

106

107 Between 10 000 and 11 000 cal. a BP the ice sheet margin in west Greenland began
108 to retreat inland from a position near the present coastline (Funder 1989). The local
109 marine limit is likely to be slightly higher than 40 ± 5 m a.s.l. (Storms *et al.* 2012) and this
110 is an important note in this study because any shorelines much above this altitude are thus
111 related to palaeolakes. The general retreat was punctuated by numerous still-stands, or
112 perhaps minor readvances, which left a series of large-scale and near-continuous sinuous
113 and lobate major moraine systems across west Greenland, as classified, dated and named
114 by Ten Brink & Weidick (1974), Ten Brink (1975), van Tatenhove *et al.* (1996), and Levy
115 *et al.* (2012) (Fig. 1). Further insights into the geochronology and landscape evolution of
116 the Kangerlussuaq-Russell Glacier area have been gained by analyses of lake sediments
117 (Eisner *et al.* 1995; Aebly & Fritz 2009; Anderson & Leng 2004; Young & Briner 2013,
118 2015) and valley fill sediments (Storms *et al.* 2012). The most recent consensus is that
119 the Fjord moraine system (not shown on figure 1) dates to 8340 – 9080 cal. a BP, the
120 Umîvît moraine system to 7360 to 7960 cal. a BP, the Keglen moraine system to 6490 to
121 7190 cal. a BP, and the Ørkendalen moraine system to 6400 to 7030 cal. a BP (Storms *et*
122 *al.* 2012, Fig. 1). The landscape in the area of this study (Fig. 1) therefore represents the
123 mid-Holocene and <1000 years of evolution during deglaciation.

124

125 Between 4200 and 1800 cal. a BP the ice sheet margin was (an unknown distance)
126 farther inland from the present position (Young & Briner 2013, 2015), but at Russell
127 Glacier a neoglacial advance at 2000 cal. a BP closely corresponds in position to Little Ice
128 Age moraines and to the position of the present ice margin (Forman *et al.* 2007).

129

130 Concomitant with this general ice margin retreat, the Kangerlussuaq – Russell
131 Glacier area landscape has developed as a geomorphological record of that activity. Ten
132 Brink (1975) suggested that excellent landform preservation in the area is due to the fact
133 that in this region the ice advanced up-slope. Additionally, the semi-arid climate and
134 generally stable bedrock (Aaltonen *et al.* 2010) means that mass movements are limited
135 in type and number and frequency and mostly to river banks. Furthermore, surface water
136 drainage is limited so major channels pertain to different environmental conditions than

137 at present. Consequently, soil development has been slow and thus soil cover is very thin
138 (Ozol & Brull 2005) permitting bedrock form to remain visible especially via aeolian
139 deflation. Vegetation cover is limited and so where sediments and depositional landforms
140 do exist their morphology is clear and their bulk composition can be relatively easily
141 inferred from natural exposures such as aeolian deflation cusps and hollows.

142

143 **Datasets and methods**

144 In this study we obtained and corrected fine-resolution (2 m grid) topography data,
145 compiled existing geological information and created our own landcover (30 m grid)
146 classification. These datasets and our methodology are described and explained in the
147 [Supporting Information](#). These datasets in combination and with our own field studies
148 enabled creation of a digital geomorphological map of the Kangerlussuaq – Russell
149 Glacier area. Our scrutiny of the landforms included development of novel digital
150 analyses.

151

152 *Glacial geomorphology*

153 Our glacial geomorphology map was compiled by firstly creating a geodatabase of
154 existing geomorphological data, most notably the ‘major moraine systems’ originally
155 mapped by Ten Brink (1975) but developed in terms of chronology by van Tatenhove *et*
156 *al.* (1996) and Storms *et al.* (2012). None of these previous efforts completely cover the
157 area considered in this study ([Fig. 1](#)) and none at a fine-resolution. Additionally, a
158 geomorphological assessment of part of the Leverett Glacier ice margin by Scholz &
159 Baumann (1997) was used, as were Little Ice Age (LIA) and neoglacial landforms by
160 Forman *et al.* (2007), some parts of the Ørkendalen moraines by Levy *et al.* (2012), and
161 aeolian landforms by Willemse *et al.* (2003). Lidberg (2011) reported a wealth of field
162 photographs, description and reasoned interpretation of the glacial geomorphology of a
163 part of the area considered in this study. Secondly, we primarily utilised our topography
164 data set ([Fig. 1](#)), but with reference of that to our geological ([Fig. 2](#)) and land cover
165 datasets ([Fig. 3](#)), to extend and infill this previous mapping with our identification of
166 glacial geomorphology. Mapping was supported by field observations and the authors’
167 own oblique aerial photographs both spanning multiple years from 1985 to 2015.

168

169 Mapping of glacial geomorphology focussed on remotely identifying:

- 170 (i) Moraine ridges to interpret the position and probable style of ice margin advances
171 (or still-stands but they are far less likely in this area: Ten Brink 1975) of the ice
172 margin.
- 173 (ii) Till/drift mantle/veneer distribution, and kame and kettle topography (Ten Brink
174 1975) so as to refine suggestions of active ice margin retreat versus ice stagnation
175 – disintegration, respectively.
- 176 (iii) Palaeochannels to interpret past meltwater routing and style.
- 177 (iv) Spillways to identify major meltwater routes between adjacent valleys.
- 178 (v) Shorelines to determine the presence and extent of former lakes and the likely
179 dam type or associated ice margin configuration.
- 180 (vi) Perched fans and deltas, braidplains and marine terraces, as marked by sloping
181 and horizontal terrace edges, respectively, to identify changes in meltwater-
182 sediment discharge regime and/or changes in base level.

183 For each of these categories criteria including position and association, shape and size
184 and texture were used to discern landforms (Table 1). Since this study encompasses such
185 a large area that is relatively remote and inaccessible, virtually all of our
186 geomorphological information is derived from the fine-resolution topography and from
187 superficial landform character as represented in the topography, geology and landcover
188 maps. This meant that assessing whether a particular ridge or hummock was bedrock or
189 sedimentary depended on multiple enquiries. Firstly, its context (what else was in its
190 vicinity) was considered. For example multiple gully heads at a similar elevation on a
191 hillslope could indicate a change in substrate hardness. Secondly, its form was
192 considered. For example bedrock hummocks in the area tend to have at least one steep
193 side, owing to the geological inclination and dip, whereas especially older moraine ridges
194 tend to be much more subdued forms. Thirdly, its texture was informative. Comparison
195 between the DEM and the landcover map showed that grasses and sedges appeared
196 ‘smooth’ on the DEM and indicated soil and thus sediments, whereas bare rock was
197 visually rough. Bedrock areas could also be detected with geological structure (faults,
198 cracks, lineations), ‘stoss and lee’ hummocks and superimposed isolated boulders.

199

200 Use of these criteria (Table 1) was aided by digital topographic analysis, such as
201 interactively taking vertical transects off the DEM, analysis of departures in elevation
202 from a local trend to quantify local landform relief, visual assessment of hillshaded

203 images especially for surface texture, for example (Fig. 4A, B, C, D, respectively), 3D
204 visualisation (Fig. 5) and field photographs (Fig. 6). Regarding detrending, we generally
205 used the ArcGIS 10.2 tool 'focal statistics' (with calculation of 'mean' elevation in a
206 circular moving window) because the typical width of moraine ridges in the area is 40 to
207 60 m and the typical width of palaeochannels is 10 to 20 m. Palaeolake shorelines, which
208 in this study area do not contain any record of glacio-isostatic uplift, were digitally drawn
209 using the 'create contour' function in the 3D Analyst extension of ArcGIS 10.1. Terraces
210 were mapped and queried for elevation at the boundary/edge between the sloping riser
211 and the relatively flat tread morphological units. Horizontal terrace edges identified
212 incised fluvial floodplains/braidplains and incised marine terraces, and sloping terrace
213 edges identified incised glacial fans and deltas. Variations in spatial density,
214 orientation and geometry were computed via export of landform centroid coordinates
215 and attributes to a text file.

216

217 **Results and interpretation**

218 A total area of ~1200 km² was mapped for its glacial geomorphology and included 2076
219 'moraine' polygons, 428 palaeochannels, 261 terrace edges, 24 deltaic- or fan-shaped
220 landforms and several streamlined bedrock hummocks (Fig. 7). A .pdf version of this map
221 enabling zoom and pan functions and with layers that can be switched on and off is
222 available as [Supporting Information \(Fig. S7\)](#). Moraine ridges on plateau areas and those
223 that cross valley floors (Fig. 5A) are generally aligned north-south, i.e. transverse to
224 regional slope, and comprise sinuous ridges typically with 5 m local relief (Fig. 7). They
225 are also sparsely-spaced; typically the distance between the ridges is approximately ten
226 times the width of the ridge (Fig. 5A, D). Moraine ridges on valley sides often occur in sub-
227 parallel stacks and with direct association of minor palaeochannels (Fig. 5A, 7), so are
228 most likely moraine-kame terrace complexes (Weidick 1968; Ten Brink 1975) reflecting
229 re-working by meltwater of moraine during progressive ice margin retreat and thinning.
230 Overall, the moraines mapped in this study exhibit considerable complexity in planform
231 and have asymmetry in position across local valleys and across adjacent hillsides and
232 local plateaux (Fig. 7). The complexity and asymmetry of these moraine ridges and their
233 occurrence both within and between the previously identified 'major moraine complexes'
234 means that only local (e.g. for a single valley), not regional ice margin retreat patterns are
235 distinguishable in our mapping (Fig. 7).

236

237 Nonetheless, on an individual landform basis the moraines mapped in this study
238 closely correspond to those mapped by Ten Brink (where there is overlap with his Plate
239 2 and our study area) but in general we identify at least an order of magnitude more
240 ridges. Discrepancy in position between our moraines and Ten Brink's (1975) could be
241 due to Ten Brink's use of aerial photographs that had not been orthorectified, as hinted
242 at by the 'approximate scale' label on his maps. Discrepancy between the number of
243 moraine ridges that we identify and those by Ten Brink (1975) is due partly to the higher
244 resolution of the data we have to hand, and partly due to the rigid criteria imposed by
245 Ten Brink (1975) that only moraines that extended continuously for several kilometres
246 and only those in similar topographic positions on both sides of valleys were included.

247

248 Furthermore, whilst Ten Brink was motivated to identify large-scale ice margin
249 advances, we are interested in revealing the detail and complexity of ice margin
250 dynamics, and in particular the nature of meltwater at the ice margin. With this interest
251 in mind, and targeting where local cross-cutting relationships or else direct contact
252 between moraines and meltwater landforms exist, we describe in detail four sub-areas of
253 our map, informally named here as the 'western spillway', the area around Aajuitsup
254 Tasia, a gorge emanating from the Leverett Glacier proglacial area, and the Ørkendalen
255 valley (Fig. 7). The central part of our study area immediately to the north of Aajuitsup
256 Tasia contains evidence for multiple palaeolakes, multiple shorelines of these
257 palaeolakes, and exchange of water between them via spillways. The southern part
258 including the Sandflugtdalen (Akuliarusiarsuup Kuua) and Ørkendalen (Qinnguata
259 Kuusua) valleys (Fig. 1) includes recessional moraines and extensive suites of ice
260 marginal channels. For brevity we only describe herein the geomorphology of the four
261 sub-areas that we then go on to discuss.

262

263 *Western spillway*

264 The 'western spillway' (Fig. 8) exits into a local valley known as Ringsødal and comprises
265 a 40 to 60 m deep and ~250 m wide gorge with sub-linear planform and a v-shaped cross-
266 section. The floor of the gorge at 295 m a.s.l. contains bedrock hummocks with a
267 streamlined planform and steep (cliff) sides. A major palaeolake fed into this spillway as
268 evidenced by a very distinct shoreline at 340 m a.s.l (Fig. 8). This shoreline is altitudinally

269 far above the local marine limit and is open-ended meaning that the dam for the lake
270 water no longer exists. For the lake to form a shoreline 45 m above the spillway floor, the
271 spillway must not have existed during lake formation. A moraine dam could have existed
272 at the northern (inlet) end of this spillway (see black arcs and question marks in Fig. 8)
273 but whether failure of this possible dam was the mechanism of formation of the spillway
274 remains ambiguous; but it can be said that the streamlined bedrock hummocks support
275 an outburst flood hypothesis. For note, all of the moraines in the 'western spillway' area
276 (Fig. 8) are likely to belong to the Umîvît moraine system, dating to 7360 to 7963 cal. a
277 BP since they broadly match the extent of that moraine system as presented by Storms et
278 al. (2012; Fig. 1).

279

280 *North of Aajuitsup Tasia*

281 The area immediately to the north of Aajuitsup Tasia, including that known locally as
282 'Maniitsoq', contains: (i) several laterally-extensive and horizontal benches on multiple
283 valley sides and these are shorelines at 292 m a.s.l. and 312 m a.s.l. (Fig. 6A) (ii) cols
284 between these valleys with a box-shaped cross-section and with a floor with mean
285 elevation 300 m.asl, i.e. between these two shorelines and thus indicative of a spillway
286 (Fig. 9), (iii) fan-shaped deposits with an apex situated at the spillway exits, usually with
287 a steep down-slope edge, often with incised gullies set into this edge (Figs 5B, 9), and (iv)
288 sub-parallel > 5 m local relief ridges with arcuate crests trending transverse to
289 (palaeo)ice flow and in direct contact with shorelines but situated (only) in elevation
290 below the shorelines (Figs 5C, 6A). These sub-parallel low-relief ridges are
291 topographically and geomorphologically analogous to the arcuate moraines described on
292 Baffin Island by Andrews & Smithson (1966) and are most likely De Geer moraines (c. f.
293 Lindén & Möller 2005).

294

295 The Aajuitsup Tasia – Sanninasoq valley and palaeolake(s) apparently received
296 meltwater from numerous sources, including directly from the Russell Glacier ice margin
297 and from meltwater draining over at least two cols (Figs 6B, 9), i.e. spillways. A fan-
298 shaped landform on the slopes immediately to the south and altitudinally beneath each
299 spillway indicates sedimentation into a lacustrine environment from debris-charged
300 meltwater routing over the spillways (Fig. 5C). Therefore the Aajuitsup Tasia –

301 Sanninasoq valley palaeolake(s) were contemporaneous with meltwater routing through
302 the two spillways.

303

304 This entire valley has a reverse bed gradient (i.e. towards the east) so the deepest
305 part of any palaeolake (at ~50 m) was towards the present ice margin. This depth of
306 water and this reverse bed gradient means that palaeolake(s) in this valley were likely
307 ice-dammed at the easternmost end and by an advanced Russell Glacier terminus. The
308 reverse bed gradient also explains why this valley holds such well-preserved moraines
309 on the valley floor, because erosion by (late Holocene) meltwater and submergence by
310 (late Holocene) sedimentation has not occurred, in contrast to other neighbouring valleys
311 where moraines are predominantly preserved on valley sides.

312

313 *South of Leverett Glacier proglacial area*

314 The southernmost extent of the Leverett (palaeo-)proglacial area (Figs 6B, 6C) connects
315 to the Ørkendalen valley via an impressive 4.2 km long gorge (Fig. 5D). This gorge drops
316 >200 m in elevation and has slopes of up to 105 and 55 m high on the northern and
317 southern sides, respectively (Fig. 10 inset). Several inflexions in the northern side slopes
318 may be associated with a palaeosurface on the southern side (Fig. 10 inset). Indeed in the
319 lower part of the gorge, where it broadens to >400 m wide, several (discordant) terrace
320 flights occur. These flights indicate sedimentation with a higher base level (altitudinally
321 far above palaeo-sea levels), which was most likely due to the presence of the Ørkendalen
322 valley glacier effectively blocking the southernmost part of the gorge. Indeed the wider
323 southern part of the gorge is within the outer limit of Ørkendalen lateral moraines (Fig.
324 10). It is ambiguous as to whether the gorge head has been overridden or infilled by
325 moraine and glacialfluvial sediment. Therefore this gorge could either be contiguous with,
326 or could pre-date, the most extensive ice margin of the Leverett Glacier between 6406
327 and 7028 cal. a BP (Storms *et al.* 2012). The 2.7 km broad and 600 m long fan of sediment
328 at the mouth of this gorge (Figs 5B, 10) has a relief of just 33 m and such a low-relief fan
329 slope indicates relatively fine-grained deposition from fluidal flows.

330

331 *The Ørkendalen valley*

332 The Ørkendalen valley is notable for numerous stacked sequences of sub-parallel ridges
333 that each have crests with alignment that is sub-parallel to local topographic contours

334 (Fig. 11). The ridge crests are typically 5 to 10 m but occasionally >15 m above the local
335 (detrended) surface. Topographically, these moraine ridges can be partially
336 distinguished from each other and from the surrounding hillslopes by minor
337 palaeochannels (Fig. 11). These palaeochannels tend to be relatively small (<20 m in
338 cross-section) and occur in especially well-developed series on valley sides. Larger
339 palaeochannels (tens of metres in cross-section) are isolated features and have greater
340 sinuosity than the smaller channels. Some of the larger palaeochannels have an
341 anastomosing planform and some have an undulating long-profile, all of which is
342 indicative of subglacial channels (Greenwood *et al.* 2016), at least partially in bedrock.
343 Specifically, we interpret that these channels represent a sub-marginal setting where ice
344 surface drainage reached the bed through thin (a few tens of metres) ice (c. f. Margold *et*
345 *al.* 2013). These local landform assemblages are therefore most likely moraine-kame
346 terrace complexes (Weidick 1968; Ten Brink 1975) and they record progressive thinning
347 and retreat of the Ørkendalen valley glacier over ~1000 years.

348

349 **Discussion**

350 *Moraine types*

351 An absence of steep rock walls surrounding the ice sheet margin, the generally massive
352 and hard crystalline geology of the region, and the aridity of the climate means that during
353 the mid-Holocene, as at present, frost weathering and thus accumulation of supraglacial
354 debris was very restricted. Consequently the mapped moraines are probably composed
355 of debris that has melted-out from basal ice, as has been described in this study area for
356 contemporary and LIA moraines by Knight *et al.* (2002), Adam and Knight (2003) and
357 Forman *et al.* (2007). The mapped position, spatial arrangement and geometry of
358 individual ridges can be used to suggest three distinct moraine types. Characterisation of
359 different types of moraines based on fine-resolution topography is absent from the
360 Greenland literature and yet is important given a lack of opportunity for sedimentological
361 analyses due the problems with accessing this terrain.

362

363 Sparsely-spaced and discontinuous moraine ridges with irregular and sinuous planform,
364 with undulating and relatively sharp-crested ridges, with symmetrical cross-sectional
365 shape and situated on plateaux and less commonly on valley sides are most likely to be
366 end moraines. Specifically, this geometry and geomorphology suggests that they are

367 probably push and squeeze moraines and thus they are analogous to the moraines along
368 the present-day northern flank of Russell Glacier (Knight *et al.* 2002, Adam & Knight
369 2003). The present-day moraines are possibly of larger dimensions than those of the mid-
370 Holocene because they are accretions from several advances (Forman *et al.* 2007). These
371 types of moraines develop incrementally over multiple seasons and may relate to
372 episodes of glacier thickening (Evans & Heimstra 2005) but we acknowledge that
373 sedimentological information is required to unravel the exact sequence of formational
374 processes.

375

376 Mapped multiple ridges that are closely-spaced, sub-parallel and often in
377 concentric arcs, are restricted to positions on wide and low-angle valley floors,
378 specifically the Leverett Glacier proglacial area and at the westernmost extent of several
379 of the lakes north of Aajuipsup Tasia (Fig. 9). They tend to have asymmetric cross-
380 sections. They are thus most likely to be composite ridges, or thrust-block moraines and
381 suggest compressive (ice advance) interaction of the glacier terminus with frozen ground
382 and results in subglacial sediment becoming elevated (Hambrey & Huddart 2006). This
383 processes will be greatly facilitated where a glacier is flowing uphill out of an
384 overdeepening, as at Leverett Glacier (see maps in Morlighem *et al.* 2013), or onto a
385 locally-inverse bed slope such as at the westernmost extent of several of the lakes north
386 of Aajuipsup Tasia (Fig. 9).

387

388 At the easternmost end of Aajuitsup Tasia the mapped moraines are situated
389 below the altitude of palaeo-lake levels and if they are contemporaneous with the
390 shorelines, which they seem to be due to an apparent direct physical contact, then they
391 are most likely De Geer moraines (De Geer 1889; Lindén & Möller 2005). De Geer
392 moraines are indicative of grounded ice margin retreat within a water body; in this case
393 an ice marginal lake. The most eastward De Geer moraine corresponds in position to the
394 most eastward extent of shoreline(s), hence it is apparent that a grounded Russell Glacier
395 ice margin retreated eastwards progressively into deeper water and that this water was
396 impounded at its easternmost end by an ice-dam.

397

398 ***Meltwater landform formation***

399 The palaeoglaciological significance of the moraines and meltwater landforms mapped
400 in this study concern ice margin position(s) and meltwater dynamics, respectively,
401 although these two sets of conditions are spatio-temporally inter-related. Meltwater
402 landforms have often been used with ice-marginal landforms to infer past ice sheet
403 geometry and dynamics, and these interpretations are necessarily based on relatively
404 simple assumptions regarding landform formation (Greenwood *et al.* 2016). In
405 contrast, inference of palaeo-hydrological systems using meltwater landforms are much
406 less common and usually target prominent landform-assemblages such as eskers and
407 tunnel valleys; recent examples include Nitsche *et al.* (2013), Phillips & Lee (2013),
408 Storrar *et al.* (2014), Burke *et al.* (2015), Lee *et al.* (2015) and Livingstone *et al.*
409 (2015).

410

411 The overwhelming signature of meltwater activity during the mid-Holocene in
412 this part of west Greenland is that related to proglacial meltwater, in the form of ice
413 marginal lakes, perched deltas into these lakes, spillways feeding, connecting and
414 draining these lakes, perched fans and glacifluvial terraces. Most of this landform
415 evidence can be explained by hypothesis of normal ice ablation-fed river flows.
416 However, some evidence such as box canyons and streamlined bedrock mounds,
417 together with consideration of the necessary dam to impound the lake water, has
418 suggested high-magnitude glacier outburst flood ('jökulhlaup') activity (c.f. Carrivick *et al.*
419 *al.* 2004; Carrivick 2007). Evidence of a dynamic and varied proglacial runoff routing
420 and style during the mid-Holocene, and a likely direct association of this with ice margin
421 dynamics, comes from the multiple shorelines around several of the (probably ice-
422 dammed) palaeolakes (Carrivick & Tweed 2013). Specifically, a shoreline has to be
423 formed where lake levels are relatively stable, and if the lake was ice-dammed, that
424 requires a quasi-stable ice dam thickness.

425

426 The hundreds of minor palaeochannels that exist in stacked successions
427 throughout the study area and that are particularly pervasive in the Ørkendalen valley
428 (Fig. 11) delineate progressive recession and thinning of the ice margin. In direct
429 association with kame terraces, these channels illustrate drainage of supraglacial
430 meltwater along the mid-Holocene ice margin, especially where ice has been pinned
431 against a topographic slope (c. f. Kleman *et al.* 1992; Dyke, 1993; Greenwood *et al.*

432 2007; Margold *et al.* 2013). The fact that the larger (up to a few tens of metres wide) of
433 these lateral channels are apparently at least partially cut into bedrock means that they
434 probably represent former subglacial drainage routeways and thus should be
435 considered to be submarginal channels, i.e. formed at the lateral margin but beneath the
436 ice surface (c. f. Greenwood *et al.* 2007; Syverson & Mickelson 2009; Lovell *et al.* 2011;
437 Margold *et al.* 2011, 2013b). For comparison, the contemporary ice margin on the
438 northern flank of Russell Glacier is known to hold a submarginal channel that connects
439 the large ice-dammed lake with 'overspill lake 1' (Russell *et al.* 2011). Palaeochannels
440 with a distributary arrangement (e.g. Fig. 5B) are not concordant with moraines in
441 position or orientation, so do not correspond to likely former ice margins and therefore
442 could mark former minor subglacial channels.

443

444 Lateral channels have usually be attributed to cold-based ice margins, where
445 percolation of meltwater in inhibited (Kleman *et al.* 1992; Dyke 1993; Kleman &
446 Borgström 1996). The pervasive and dominant character and widespread distribution
447 of lateral and submarginal meltwater channels in this study is similar to that found in
448 parts of Scandinavia, the Canadian Arctic and the North American Cordillera, where
449 cold-based or polythermal ice prevailed during deglaciation (Kleman *et al.* 1992; Dyke
450 1993; Sollid & Sørbel 1994). The relative paucity of landform evidence of *subglacial*
451 meltwater in this study suggests that this part of the west Greenland ice sheet did not
452 have a widely developed subglacial hydrological system during the mid-Holocene. An
453 apparent lack of a developed subglacial hydrological system is not at all unusual in
454 considerable parts of ice sheets (Kleman & Glasser, 2007) and together with the
455 relatively ubiquitous lateral meltwater channels, can most simply be explained if the ice
456 were cold-based or polythermal (c. f. Kleman *et al.* 1992; Dyke 1993; Sollid & Sørbel
457 1994).

458

459 ***Controls on spatial distribution of landforms***

460 The spatial pattern of moraine ridges, palaeochannels and kame terraces across our
461 study area is relatively coherent, with no quantifiable (statistically significant) change in
462 spatial density, orientation or geometrical size of landforms, such as along the entire
463 length of Ørkendalen (Fig. 11). Therefore, and in terms of the moraines, ice margin
464 retreat has apparently been consistent in style for a time period of hundreds to

465 thousands of years. In terms of meltwater, we find that the geological legacy of runoff
466 generation, routing and magnitude-frequency style changed little for ~1000 years
467 during the mid-Holocene. This uniformity of geomorphological evolution due to
468 meltwater runoff contrasts with that during the Laurentide Ice Sheet deglaciation
469 (Storrar *et al.* 2014) and can tentatively be attributed to a lack of abundant sediment
470 and to a lack of subglacial bed-channel coupling if compared with the historical
471 (decadal-scale) landform evolution at Breiðamerkurjökull, for example (Storrar *et al.*
472 2015).

473

474 The asymmetric distribution of moraines within major moraine complexes, such
475 as between the contemporary termini of Russell Glacier and Isunnguata Sermia (Fig. 7)
476 is probably due to glaciers in troughs having very different dynamics to that part of the
477 ice margin situated at higher elevation between valleys, and on the timescales of tens to
478 hundreds of years. Such a control of local topography on local ice sheet terminii is
479 similar to that interpreted for the Canadian Arctic Archipelago (Storrar *et al.* 2014) and
480 has been noted by Weidick *et al.* (2012) for the Nuup Kangerlua region in southern
481 West Greenland. It is also evident from contemporary ice surface velocity
482 measurements (e.g. Palmer *et al.* 2011; Morlighem *et al.* 2013) and ice margin retreat
483 rates in this part of west Greenland.

484

485 The small portions of the landscape that we find in this study with a till/drift
486 mantle/veneer (Fig. 6D) that is indicative of subglacial deposition probably represent
487 transition from an actively retreating ice margin to a more complex and stagnant ice
488 body (c. f. Margold *et al.* 2013). A present-day example of this transitional situation is
489 shown in Figure 6E. Further support for the idea that this part of the west Greenland ice
490 sheet was active throughout its mid-Holocene retreat perhaps comes from the absence
491 of eskers. Eskers tend to be a key focus of glacial geomorphology-based studies on ice
492 sheet margins and are common at other ice sheet margins (e.g. Brennand 1994; Clark &
493 Walder 1994; Winsborrow *et al.* 2010). However, mindful that eskers have been
494 associated with active ice margin retreat in Iceland (e.g. Evans & Twigg 2002) other
495 factors additional to ice flow are likely to have been important in west Greenland in the
496 mid-Holocene for restricting esker formation. We consider that such other factors
497 include a distributed meltwater drainage system (c. f. Livingstone *et al.* 2015) and

498 restricted sediment supply due to a lack of supraglacial debris and due to a cold-based
499 subglacial thermal regime, as described and interpreted earlier in this study,
500 respectively. Additionally, a lack of deformable sediment could explain the lack of
501 eskers (Burke *et al.* 2015) but both factors are contrary to the contemporary situation
502 in this part of west Greenland (e.g. Russell *et al.* 2011 and Adam & Knight 2003,
503 respectively).

504

505 In this study we did not find any relationship between moraine or palaeochannel
506 distribution (spatial density) and geological variability. This fact, together with the
507 presence of several major and many minor channel systems incised into the hard
508 crystalline bedrock, suggests that the mid-Holocene ice margin system in this part of west
509 Greenland was more similar to that understood for Antarctic continental shelves than
510 for the periphery of the northern hemisphere Quaternary ice sheets. Indeed Antarctic
511 continental shelf systems also have a general lack of evidence of subglacial drainage and
512 an absence of eskers (e.g. Wellner *et al.* 2006; Graham *et al.* 2009) as has been found in
513 this study. However, the Antarctic system has been suggested to have meltwater delivery
514 through small canals or a deforming till aquifer (Graham *et al.* 2009; Noormets *et al.*
515 2009) and that cannot be evaluated by this study but is intriguing in the context of west
516 Greenland and deserves careful consideration.

517

518 The northern part of our study area, along the Isunnguata Sermia valley, is
519 peculiar because any discernible glacial geomorphology is extremely sparse (Fig. 7).
520 Notwithstanding that this valley is deeper and wider there is no difference in topography
521 or geology along the Isunnguata Sermia valley in comparison to the other valleys of this
522 study we consider it useful to speculate on the major types of events that could explain
523 such a pattern. In brief, during the mid-Holocene the Isunnguata Sermia terminus could
524 have: (i) retreated very rapidly without sufficient time in any one configuration for
525 discernible moraine ridges to be deposited and for palaeochannels to develop, or (ii) any
526 moraine ridges and palaeochannels have become buried with the abundant glacial
527 sediment that is now and probably has been throughout the mid-Holocene accumulating
528 on the valley floor, as a product of ablation-fed river flows and jökulhlaups.

529

530

531 ***Regional ice margin dynamics***

532 Our mapping supports a general mid-Holocene regional eastward migration of the
533 western margin of the Greenland Ice Sheet (GrIS) from Kangerlussuaq to the Russell
534 Glacier area (c. f. Weidick 1968; Ten Brink 1975; van Tatenhove *et al.* 1996). Our mapping
535 also reveals considerably more detail in the position, size and geometry of former ice
536 margins associated with this general retreat by including not only major, contiguous,
537 advances as by Ten Brink (1975) but also minor discontinuous moraine ridges.
538 Numerous minor readvances are evidenced by the number of moraine ridges, although
539 the spatial patterns of them suggests that these ice margin advances were short-lived. A
540 low sediment supply as well as a short period of time of formation more than likely
541 explains why these moraine ridges are far smaller in local relief than those at the
542 contemporary ice margin. We have not sought to produce a qualitative reconstruction of
543 landscape evolution because we realised that there were too many ambiguities and
544 permutations, specifically that: (i) our sub-sites do not unfortunately have (cross-cutting)
545 stratigraphical evidence between them, and (ii) as discussed above considerable
546 asymmetry in (intra-complex) moraine positions is apparent across local valleys and
547 adjacent hillsides and local plateaux so simply using the dated moraine complexes to link
548 our sub-sites would be speculative at best. Such 'metachronous' problems are not
549 unusual in landform records of ice sheets and probably require strategic and cautious
550 application of an 'inversion model' to unravel them (Klemen & Borgström, 1996).

551

552 ***Regional meltwater dynamics***

553 Meltwater has left a more widespread and arguably a more pervasive landscape record
554 than deposition of sediment directly from a glacier in this study area. This landscape
555 record is dominated by landforms related to transitory proglacial meltwater systems, all
556 existing within a time period of ~1000 years, yet each with long-lasting geological legacy.
557 In particular, this evidence includes temporary storage of meltwater in large (ice-
558 dammed?) lakes such as Aajuipsup Tasia, drainage via deeply and progressively incised
559 gorges such as from the Leverett Glacier proglacial area, and progressive ice margin
560 thinning and retreat as in Ørkendalen, for example. Several major lakes (systems) must
561 have had glacier termini abutting them to form dams, and several of these lakes had
562 multiple levels probably indicating glacier thickening/thinning. The number and the
563 size(s) of the palaeolakes revealed in this study and their transitory nature is comparable

564 to the present day situation in west Greenland (Carrivick & Quincey 2014). Some lakes
565 drained via spillways, and whilst it is presently ambiguous as to whether these were lake
566 maintenance spillways or outburst flood spillways (c. f. Perkins & Brennand 2015), they
567 illustrate the exchange of water between local valleys and thus major hydrology
568 reorganisation as a response to changing ice margin configurations. The fans and deltas
569 associated with these spillways are not huge, which is to be expected because any of the
570 numerous lakes upstream would have acted as a sediment trap. The most spectacular
571 sedimentation is actually at the distal end of the gorge emanating from the Leverett
572 Glacier proglacial area and comprises sedimentation in the form of stacked sloping
573 terrace edges as well as a major distal fan (Fig. 5D). The longitudinal transition from
574 incision in proximal reaches of this gorge to sedimentation in the distal reaches is striking
575 and demonstrates a rapid attenuation of (palaeo)flow transport capacity and energy (Fig.
576 5D).

577

578 Whether the lateral and submarginal palaeochannels represent a product of
579 steady-state down-cutting by normal ice ablation-fed river flows, or else a single high
580 magnitude or multiple lower magnitude erosional events is ambiguous, not least due to a
581 lack of modern analogues of these sorts of channels (Greenwood et al. 2016). Where
582 palaeochannels persist with a distributary planform, especially on inter-valley and
583 plateaux areas, the position and nature of minor subglacial channels is suggested.
584 Although minor in individual size(s), these could have been pressurised and with ability
585 to affect ice dynamics. In contrast, whilst the larger palaeochannels mapped in this study
586 at least partially cut into bedrock and thus are associated with Nye channels (see section
587 2.2.3 of Greenwood *et al.* 2016) they are isolated and do not link topographic basins so
588 are without an obvious ability to affect major (palaeo)ice flow dynamics.

589

590 **Conclusions**

591 This study has greatly improved the spatial resolution of data and knowledge of
592 topography, geomorphology and associated geology and landcover for the Kangerlussuaq
593 – Russell Glacier area, west Greenland. These data will be useful for future work on
594 deglaciation, which is likely to continue to focus on geochronology, landscape stability
595 and development/succession. Specifically, future work in this study area should look to
596 target the previously undocumented geomorphology revealed in this study for

597 sedimentological and geochronological analysis of the composition and structure of the
598 moraines, the lake sediments and the fan-shaped deposits.

599

600 This study has distinguished push-squeeze moraines, composite block moraines
601 and De Geer moraines based on a set of topographical and geomorphological criteria
602 developed for west Greenland. These moraines record minor ice advances and perhaps
603 also some glacier terminus thickening, transport of (frozen) subglacial sediment, and
604 grounding line deposition with ice marginal lakes, respectively. Asymmetry and
605 discontinuity between intra-moraine ridges across adjacent valley hillsides and valley
606 floors is attributed to a control of local topography on former ice dynamics.

607

608 Meltwater generated from this part of the west Greenland ice sheet during the
609 mid-Holocene and likely over just ~1000 years has a legacy of landforms that reveal
610 major reorganisations of proglacial routing and of runoff frequency-magnitude regime.
611 In particular, large palaeolake systems such as the Aajuitsup Tasia complex had multiple
612 shorelines and major spillways associated with them. The lake-related spillways and
613 shorelines and dry gorges such as that emanating from the Leverett Glacier proglacial
614 area evidence a spatio-temporally dynamic proglacial hydrology. Several of the lakes are
615 on local inverse slopes and would likely have been ice-dammed and would thus have
616 exerted a control on the mid-Holocene ice margin configuration and behaviour. Hundreds
617 of minor palaeochannels have an intimate association with minor moraines on hillsides
618 and are attributed to former ice marginal or lateral channels. They record progressive ice
619 margin retreat and thinning, especially in the Ørkendalen valley, and are indicative of a
620 cold-based ice margin. The few larger channels at least partially cut into bedrock are
621 interpreted to be submarginal Nye channels. Minor palaeochannels comprise networks
622 with a distributary planform that is discordant with moraines and are most likely the
623 position of former (likely inefficient) subglacial meltwater channels.

624

625 This suite of glacial landforms perhaps has more similarity with that of Antarctic
626 continental shelves than with most northern hemisphere ice sheet margins and whilst
627 several topographical, geological and glaciological controls must have been important,
628 such as a reverse bed slope, hard crystalline rock and a cold-based ice margin,
629 respectively, a lack of sediment supply seems very evident and important.

630
631
632
633
634
635
636
637
638
639
640
641
642
643
644
645
646
647
648
649
650
651
652
653
654
655
656
657
658
659
660
661
662
663
664
665
666
667
668
669
670
671
672
673
674
675
676
677
678
679
680
681

Overall, the lack of any statistically significant difference in spatial density, and of landform size and orientation across this study site, means that the most pervasive impression given by this suite of landforms is that of considerable spatio-temporal variability of meltwater routing and runoff regime persisting for ~1000 years during the mid-Holocene, despite a relatively consistent pattern and style of ice margin retreat. Landforming events during the mid-Holocene in this part of west Greenland were very similar to those of the present day. A better understanding of the timescales involved is needed to examine whether the meltwater system re-organisations correspond to changes in ice margin dynamics or vice versa.

Acknowledgements

JLC acknowledges fieldwork funding from the School of Geography, University of Leeds, for field work in 2008, 2010, 2012 and 2015, and the Royal Institute of Chartered Surveyors (RICS) (administered via the RGS-IBG) for fieldwork in 2014 (grant no. 474: DJQ). Richard Hodgkins is thanked for his provision of the IPY07-03 airborne LiDAR data. Steve Carver assisted in fieldwork in 2012. Daniel Carrivick is thanked for his field photographs of the landscape east of Lake Fergusen and Andrew Tedstone and Neil Ross are thanked for photographs of the Leverett Glacier proglacial area. M. Winsborrow, two anonymous reviewers and Editor J. Piotrowski are thanked for their careful scrutiny and constructive criticism.

References

- Aaltonen, I., Douglas, B., Frape, S., Henkemans, E., Hobbs, M., Klint, K. E., Lehtinen, A., Liljedahl, L. C., Lintinen, P. & Ruskeeniemi, T. 2010: *The Greenland Analogue Project, Sub-project C: 2008 Field and Data Report*. Posiva Oy. 136 pp.
- Adam, W. G. & Knight, P. G. 2003: Identification of basal layer debris in ice marginal moraines, Russell Glacier, West Greenland. *Quaternary Science Reviews* 22, 1407-1414.
- Aebly, F. A. & Fritz, S. C. 2009: Palaeohydrology of Kangerlussuaq (Søndre Strømfjord), west Greenland during the last ~ 8000 years. *The Holocene* 19, 91-104.
- Anderson, N. J. & Leng, M. J. 2004: Increased aridity during the early Holocene in West Greenland inferred from stable isotopes in laminated-lake sediments. *Quaternary Science Reviews* 23, 841-849.
- Andrews, J. T & Smithson, B. B. 1966: Till fabrics of the cross-valley moraines of north-central Baffin Island, Northwest Territories, Canada. *Geological Society of America Bulletin* 77, 271-290.
- Bartholomew, I., Nienow, P., Sole, A., Mair, D., Cowton, T. & King, M. A. 2012: Short-term variability in Greenland Ice Sheet motion forced by time-varying meltwater drainage: Implications for the relationship between subglacial drainage system behavior and ice velocity. *Journal of Geophysical Research: Earth Surface* (2003–2012), 117(F3).
- Brennand, T. A. 1994: Macroforms, large bedforms and rhythmic sedimentary sequences in subglacial eskers, south-central Ontario: implications for esker genesis and meltwater regime. *Sedimentary Geology* 91, 9-55.
- Burke, M. J., Brennand, T. A. & Sjogren, D. B. 2015: The role of sediment supply in esker formation and ice tunnel evolution. *Quaternary Science Reviews* 115, 50-77.
- Carrivick, J. L. 2007: Modelling coupled hydraulics and sediment transport of a high-magnitude flood and associated landscape change. *Annals of Glaciology* 45, 143-154.

- 682
683 Carrivick, J. L. & Quincey, D. J. 2014: Progressive increase in number and volume of ice marginal lakes on the western margin of the
684 Greenland Ice Sheet. *Global and Planetary Change* 116, 156-163.
- 685
686 Carrivick, J. L., Russell, A. J. & Tweed, F. S. 2004: Geomorphological evidence for jökulhlaups from Kverkfjöll volcano, Iceland.
687 *Geomorphology* 63, 81-102.
- 688
689 Carrivick, J. L., Turner, A. G., Russell, A. J., Ingeman-Nielsen, T. & Yde, J. C. 2013: Outburst flood evolution at Russell Glacier, western
690 Greenland: effects of a bedrock channel cascade with intermediary lakes. *Quaternary Science Reviews* 67, 39-58.
- 691
692 Clark, P. U. & Walder, J. S. 1994: Subglacial drainage, eskers, and deforming beds beneath the Laurentide and Eurasian ice sheets.
693 *Geological Society of America Bulletin* 106, 304-314.
- 694
695 De Geer, G. 1889: Ändmoräner i trakten mellan Spånga och Sundbyberg. *Geologiska Föreningens i Stockholm Förhandlingar* 11, 395-
696 397
- 697
698 Donner, J. & Jungner, H. 1975: Radiocarbon dating of shells from marine Holocene deposits in the Disko Bugt area, West Greenland.
699 *Boreas* 4, 25-45.
- 700
701 Dyke, A. S. 1993: Landscapes of cold-centred Late Wisconsinan ice caps, Arctic Canada. *Progress in Physical Geography* 17, 223-247.
- 702
703 Eisner, W. R., Törnqvist, T. E., Koster, E. A., Bennike, O. & van Leeuwen, J. F. 1995: Paleoeological studies of a Holocene lacustrine
704 record from the Kangerlussuaq (Søndre Strømfjord) region of West Greenland. *Quaternary Research* 43, 55-66.
- 705
706 Evans, D. J. & Hiemstra, J. F. 2005: Till deposition by glacier submarginal, incremental thickening. *Earth Surface Processes and*
707 *Landforms* 30, 1633-1662.
- 708
709 Evans, D. J. & Twigg, D. R. 2002: The active temperate glacial landsystem: a model based on Breiðamerkurjökull and Fjallsjökull,
710 Iceland. *Quaternary Science Reviews* 21, 2143-2177.
- 711
712 Fitzpatrick, A. A. W., Hubbard, A. L., Box, J. E., Quincey, D. J., Van As, D., Mikkelsen, A. P. B., ... & Jones, G. A. 2014: A decade (2002-
713 2012) of supraglacial lake volume estimates across Russell Glacier, West Greenland. *The Cryosphere* 8, 107-121.
- 714
715 Forman, S. L., Marín, L., Veen, C., Tremper, C. & Csatho, B. 2007: Little ice age and neoglacial landforms at the Inland Ice margin,
716 Isunguata Sermia, Kangerlussuaq, west Greenland. *Boreas* 36, 341-351.
- 717
718 Funder, S. 1989: Quaternary geology of the ice-free areas and adjacent shelves of Greenland: Chapter 13 in Quaternary geology of
719 Canada and Greenland: 743-792
- 720
721 Génsbøl, B. 2004: A nature and wildlife guide to Greenland. 259 pp. Gyldendal, Copenhagen.
- 722
723 GEUS. 2013: Greenland Geological Data. Available online in a map viewer
724 <http://data.geus.dk/map2/geogreen/#Z=1&N=8148070&E=404120>. Last accessed 20/07/2015
- 725
726 van Gool, J. A., Connelly, J. N., Marker, M. & Mengel, F. C. 2002: The Nagssugtoqidian Orogen of West Greenland: tectonic evolution
727 and regional correlations from a West Greenland perspective. *Canadian Journal of Earth Sciences* 39, 665-686.
- 728
729 Greenwood, S. L., Clark, C. D. & Hughes, A. L. 2007: Formalising an inversion methodology for reconstructing ice-sheet retreat
730 patterns from meltwater channels: application to the British Ice Sheet. *Journal of Quaternary Science* 22, 637-645.
- 731
732 Greenwood, S. L., Clason, C. C., Helanow, C. & Margold, M. 2016: Theoretical, contemporary observational and palaeo-perspectives on
733 ice sheet hydrology: Processes and products. *Earth-Science Reviews* 155, 1-27.
- 734
735 Graham, A. G., Larter, R. D., Gohl, K., Hillenbrand, C. D., Smith, J. A. & Kuhn, G. (2009). Bedform signature of a West Antarctic palaeo-
736 ice stream reveals a multi-temporal record of flow and substrate control. *Quaternary Science Reviews* 28, 2774-2793.
- 737
738 Hambrey, M. J. & Huddart, D. 1995: Englacial and proglacial glaciotectonic processes at the snout of a thermally complex glacier in
739 Svalbard. *Journal of Quaternary Science* 10, 313-326.
- 740
741 Harper, J., Humphrey, N., Pfeffer, W. T., Brown, J. & Fettweis, X. 2012: Greenland ice-sheet contribution to sea-level rise buffered by
742 meltwater storage in firn. *Nature* 491, 240-243.
- 743
744 Humlum, O., Christiansen, H.H., Hansen, Hasholt, B., Jakobsen, B.H., Nielsen, N. & Rasch, M. 1995: Holocene landscape evolution in
745 the Mellemfjord area, Disko Island, Central West Greenland: area presentation and preliminary results. *Geografisk Tidsskrift-Danish*
746 *Journal of Geography* 95, 28-41.
- 747
748 Ingólfsson, Ó., Frich, P., Funder, S. & Humlum, O. 1990: Paleoclimatic implications of an early Holocene glacier advance on Disko
749 Island, West Greenland. *Boreas* 19, 297-311.
- 750
751 Kleman, J. & Borgström, I. 1996: Reconstruction of palaeo-ice sheets: the use of geomorphological data. *Earth Surface Processes and*
752 *Landforms* 21, 893-909.
- 753
754 Kleman, J. & Glasser, N. F. 2007: The subglacial thermal organisation (STO) of ice sheets. *Quaternary Science Reviews* 26, 585-597.
- 755

- 756 Kleman, J., Borgström, I., Robertsson, A. M. & Lilliesköld, M. 1992: Morphology and stratigraphy from several deglaciations in the
757 Transtrand Mountains, western Sweden. *Journal of Quaternary Science* 7, 1-17.
758
- 759 Knight, P. G., Waller, R. I., Patterson, C. J., Jones, A. P. & Robinson, Z. P. 2002: Discharge of debris from ice at the margin of the
760 Greenland ice sheet. *Journal of Glaciology* 48, 192-198.
761
- 762 Klint, K.E.S., Engström, J., Parmenter, A., Ruskeeniemi, T., Liljedahl, L.C. & Lehtinen, A. 2013: Lineament mapping and geological
763 history of the Kangerlussuaq region, southern West Greenland. GEUS. *Geological Survey of Denmark and Greenland Bulletin* 28, 57-
764 60. Open access: www.geus.dk/publications/bull
765
- 766 Lee, J. R., Wakefield, O. J., Phillips, E. & Hughes, L. 2015: Sedimentary and structural evolution of a relict subglacial to subaerial
767 drainage system and its hydrogeological implications: an example from Anglesey, north Wales, UK. *Quaternary Science Reviews* 109,
768 88-110.
769
- 770 Levy, L. B., Kelly, M. A., Howley, J. A. & Virginia, R. A. 2012: Age of the Ørkendalen moraines, Kangerlussuaq, Greenland: constraints
771 on the extent of the southwestern margin of the Greenland Ice Sheet during the Holocene. *Quaternary Science Reviews* 52, 1-5.
772
- 773 Lidberg, W. 2011: Deglaciationen av ett område på västra Grönland. Unpublished thesis. Umeå University.
774
- 775 Lindén, M. & Möller, P. 2005: Marginal formation of De Geer moraines and their implications to the dynamics of grounding-line
776 recession. *Journal of Quaternary Science* 20, 113-133.
777
- 778 Livingstone, S. J., Storrar, R. D., Hillier, J. K., Stokes, C. R., Clark, C. D. & Tarasov, L. 2015: An ice-sheet scale comparison of eskers with
779 modelled subglacial drainage routes. *Geomorphology* 246, 104-112.
780
- 781 Lloyd, J. M., Park, L. A., Kuijpers, A. & Moros, M. 2005: Early Holocene palaeoceanography and deglacial chronology of Disko Bugt,
782 west Greenland. *Quaternary Science Reviews* 24, 1741-1755.
783
- 784 Long, A. J. & Roberts, D. H. 2002: A revised chronology for the 'Fjord Stade' moraine in Disko Bugt, west Greenland. *Journal of*
785 *Quaternary Science* 17, 561-579.
786
- 787 Long, A. J., Roberts, D. H. & Dawson, S. 2006: Early Holocene history of the west Greenland Ice Sheet and the GH-8.2 event.
788 *Quaternary Science Reviews* 25, 904-922.
789
- 790 Margold, M., Jansson, K. N., Kleman, J., Stroeven, A. P. & Clague, J. J. 2013: Retreat pattern of the Cordilleran Ice Sheet in central
791 British Columbia at the end of the last glaciation reconstructed from glacial meltwater landforms. *Boreas* 42, 830-847.
792
- 793 Mernild, S. H., Liston, G. E., Hiemstra, C. A., Christensen, J. H., Stendel, M. & Hasholt, B. 2011: Surface Mass Balance and Runoff
794 Modeling Using HIRHAM4 RCM at Kangerlussuaq (Søndre Strømfjord), West Greenland, 1950-2080. *Journal of Climate* 24, 609-623.
795
- 796 Mernild, S. H., Hanna, E., McConnell, J. R., Sigl, M., Beckerman, A. P., Yde, J. C., Cappelen, J., Malmros, J. K. & Steffen, K. 2015: Greenland
797 precipitation trends in a long-term instrumental climate context (1890-2012): evaluation of coastal and ice core records.
798 *International Journal of Climatology* 35, 303-320.
799
- 800 Morlighem, M., Rignot, E., Mouginot, J., Wu, X., Seroussi, H., Larour, E. & Paden, J. 2013: High-resolution bed topography mapping of
801 Russell Glacier, Greenland, inferred from Operation IceBridge data. *Journal of Glaciology* 59, 1015-1023.
802
- 803 Nitsche, F. O., Gohl, K., Larter, R. D., Hillenbrand, C. D., Kuhn, G., Smith, J. A., ... & Jakobsson, M. 2013: Paleo ice flow and subglacial
804 meltwater dynamics in Pine Island Bay, West Antarctica. *The Cryosphere* 7, 249-262.
805
- 806 Noh, M. J. & Howat, I. M., 2015: Automated stereo-photogrammetric DEM generation at high latitudes: Surface Extraction from TIN-
807 Based Search Minimization (SETSM) validation and demonstration over glaciated regions, *GIScience and Remote Sensing*,
808
- 809 Noormets, R., Dowdeswell, J. A., Larter, R. D., Cofaigh, C. Ó. & Evans, J. 2009: Morphology of the upper continental slope in the
810 Bellingshausen and Amundsen Seas—Implications for sedimentary processes at the shelf edge of West Antarctica. *Marine Geology*
811 258, 100-114.
812
- 813 Ozols, U. & Broll, G. 2005: Soil Ecological Processes in Vegetation Patches of Well Drained Permafrost Affected Sites (Kangerlussuaq-
814 West Greenland). *Polarforschung* 73, 5-14.
815
- 816 Palmer, S., Shepherd, A., Nienow, P. & Joughin, I. 2011: Seasonal speedup of the Greenland Ice Sheet linked to routing of surface
817 water. *Earth and Planetary Science Letters* 302, 423-428.
818
- 819 Pedersen, M., Weng, W.L., Keulen, N., and Kokfelt, T.F. 2013: A new seamless digital 1:500 000 scale geological map of Greenland.
820 <http://data.geus.dk/map2/geogreen/Geology.pdf> 2013 GEUS. *Geological Survey of Denmark and Greenland Bulletin* 28, 65-68.
821
- 822 Perkins, A. J. & Brennand, T. A. 2015: Refining the pattern and style of Cordilleran Ice Sheet retreat: palaeogeography, evolution and
823 implications of lateglacial ice-dammed lake systems on the southern Fraser Plateau, British Columbia, Canada. *Boreas* 44, 319-342.
824
- 825 Phillips, E. & Lee, J. R. 2013: Development of a subglacial drainage system and its effect on glaciectonism within the polydeformed
826 Middle Pleistocene (Anglian) glacial sequence of north Norfolk, Eastern England. *Proceedings of the Geologists' Association* 124,
827 855-875.
828

- 829 Rinterknecht, V., Gorokhov, Y., Schaefer, J. M. & Caffee, M. 2009: Preliminary ^{10}Be chronology for the last deglaciation of the
830 western margin of the Greenland Ice Sheet. *Journal of Quaternary Science* 24, 270-278.
- 831
- 832 Roberts, D. H., Long, A. J., Davies, B. J., Simpson, M. J. R. & Schnabel, C. 2010: Ice stream influence on West Greenland Ice Sheet
833 dynamics during the Last Glacial Maximum. *Journal of Quaternary Science* 25, 850-864.
- 834
- 835 Russell, A. J., Carrivick, J. L., Ingeman-Nielsen, T., Yde, J. C. & Williams, M. 2011: A new cycle of jökulhlaups at Russell Glacier,
836 Kangerlussuaq, West Greenland. *Journal of Glaciology* 57, 238-246.
- 837
- 838 Scholz, H. & Baumann, M. 1997: An 'open system pingo' near Kangerlussuaq (Søndre Strømfjord), West Greenland. *Geology of*
839 *Greenland Survey Bulletin* 176, 104-108.
- 840
- 841 Storms, J. E., de Winter, I. L., Overeem, I., Drijkoningen, G. G. & Lykke-Andersen, H. 2012: The Holocene sedimentary history of the
842 Kangerlussuaq Fjord-valley fill, West Greenland. *Quaternary Science Reviews* 35, 29-50.
- 843
- 844 Storrar, R. D., Stokes, C. R. & Evans, D. J. 2014: Increased channelization of subglacial drainage during deglaciation of the Laurentide
845 Ice Sheet. *Geology* 42, 239-242.
- 846
- 847 Sugden, D. E. 1974: Landscapes of glacial erosion in Greenland and their relationship to ice, topographic and bedrock conditions. In
848 Brown, E. H. & Waters, R. S. (eds.): *Progress in Geomorphology: Papers in Honour of David L. Linton, 177-195. Institute of British*
849 *Geographers Special Publication* 7.
- 850
- 851 Sollid, J. L. & Sørbel, L. 1994: Distribution of glacial landforms in southern Norway in relation to the thermal regime of the last
852 continental ice sheet. *Geografiska Annaler. Series A. Physical Geography* 76, 25-35.
- 853
- 854 van Tatenhove, F. G., van der Meer, J. J. & Koster, E. A. 1996: Implications for deglaciation chronology from new AMS age
855 determinations in central West Greenland. *Quaternary Research* 45, 245-253.
- 856
- 857 Ten Brink, N.W. 1975: Holocene history of the Greenland ice-sheet based on radiocarbon dated moraines in West Greenland.
858 *Meddelelser om Grønland* 201, 44p.
- 859
- 860 Ten Brink, N. W. & Weidick, A. 1974: Greenland ice sheet history since the last glaciation. *Quaternary Research* 4, 429-440.
- 861
- 862 van de Wal, R. S. W., Smeets, C. J. P. P., Boot, W., Stoffelen, M., van Kampen, R., Doyle, S. H., Wilhelms, F., van den Broeke, M. R.,
863 Reijmer, C. H., Oerlemans, J. & Hubbard, A. 2015: Self-regulation of ice flow varies across the ablation area in south-west Greenland.
864 *The Cryosphere* 9, 603-611.
- 865
- 866 Warren, C. R. & Hulton, N. R. J. 1990: Topographic and glaciological controls on Holocene ice-sheet margin dynamics, central West
867 Greenland. *Annals of Glaciology*, 14, 307-310.
- 868
- 869 Weidick, A. 1968: Observations on some Holocene glacier fluctuations in West Greenland". *Meddelelser om Grønland* 165, 202 pp.
- 870
- 871 Weidick, A., Bennike, O., Citterio, M. & Nørgaard-Pedersen, N. 2012: Neoglacial and historical glacier changes around Kangarsuneq
872 Fjord in southern West Greenland. *Geological Survey of Denmark and Greenland Bulletin* 27, 68 pp.
- 873
- 874 Wellner, J. S., Heroy, D. C. & Anderson, J. B. 2006: The death mask of the Antarctic ice sheet: comparison of glacial geomorphic
875 features across the continental shelf. *Geomorphology* 75, 157-171.
- 876
- 877 Willemse, N. W., Koster, E. A., Hoogakker, B. & van Tatenhove, F. G. 2003: A continuous record of Holocene eolian activity in West
878 Greenland. *Quaternary Research* 59, 322-334.
- 879
- 880 Winsborrow, M. C., Andreassen, K., Corner, G. D. & Laberg, J. S. 2010: Deglaciation of a marine-based ice sheet: Late Weichselian
881 palaeo-ice dynamics and retreat in the southern Barents Sea reconstructed from onshore and offshore glacial geomorphology.
882 *Quaternary Science Reviews* 29, 424-442.
- 883
- 884 Young, N. E., Briner, J. P., Rood, D. H., Finkel, R. C., Corbett, L. B. & Bierman, P. R. 2013: Age of the Fjord Stade moraines in the Disko
885 Bugt region, western Greenland, and the 9.3 and 8.2 ka cooling events. *Quaternary Science Reviews* 60, 76-90.
- 886
- 887 Young, N. E. & Briner, J. P. 2015: Holocene evolution of the western Greenland Ice Sheet: Assessing geophysical ice-sheet models
888 with geological reconstructions of ice margin change. *Quaternary Science Reviews* 114, 1-17.

889

890

891

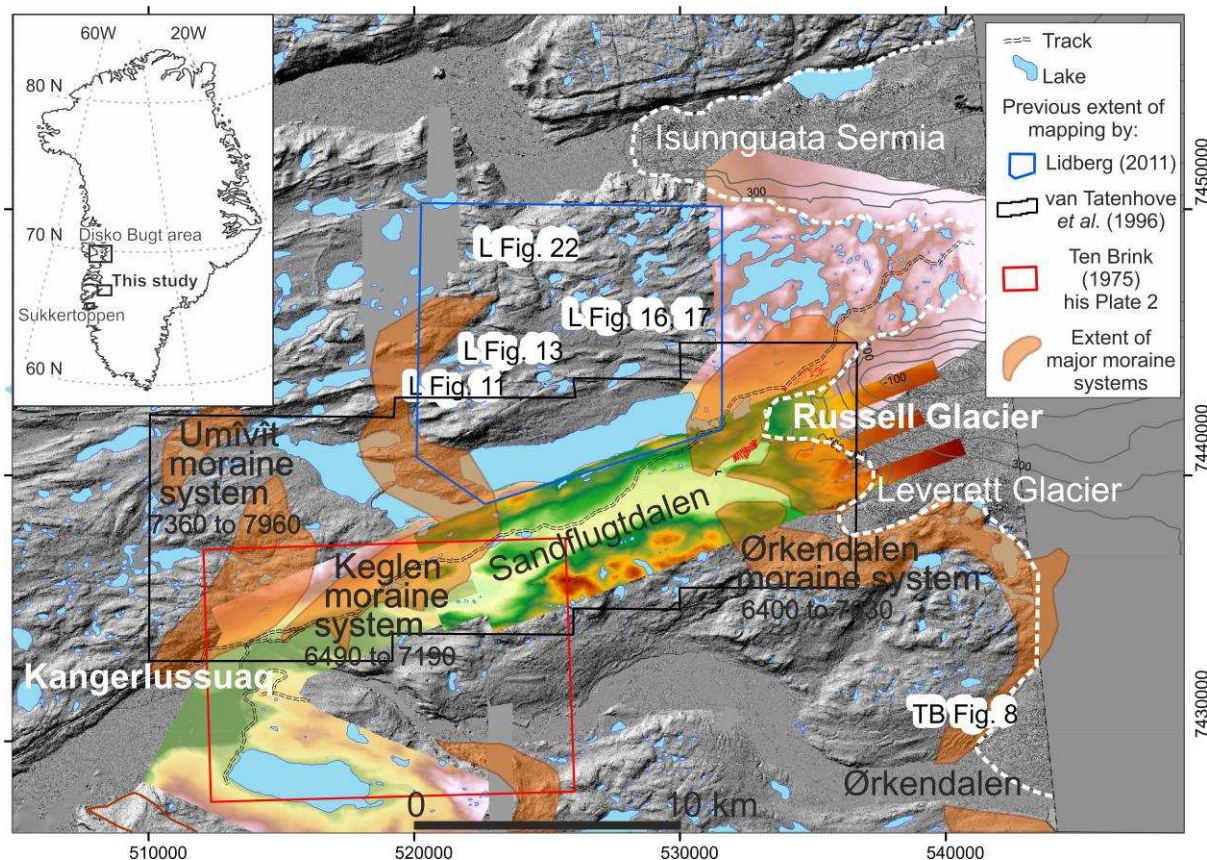
892

893

894

895 **Figure captions**

896



897

898

899 **Figure 1.** Study area, topographic data and extent of previous glacial geomorphology
 900 mapping. Topographic data includes SETSM 2 m grid DEM (b/w background), 5 m
 901 photogrammetry DEM (pastel colours), ALS 2 m DEM (vivid colours) and dGPS 3D points
 902 (red dots). ASTER DEM is not shown for clarity. Note glacier bed elevation (contours) is
 903 an extract from IceBridge data. The present day ice margin is represented by white
 904 dashed line. Field photographs by Lidberg (2011) and Ten Brink (1975) that were found
 905 to be useful to this study are geolocated on the map and with their figure numbers and
 906 with authorship denoted by 'L' and 'TB', respectively. Grid coordinates are in UTM zone
 907 22N format and dates pertaining to major moraine complexes are in cal. a BP.

908

909

910

911

912

913

914

915

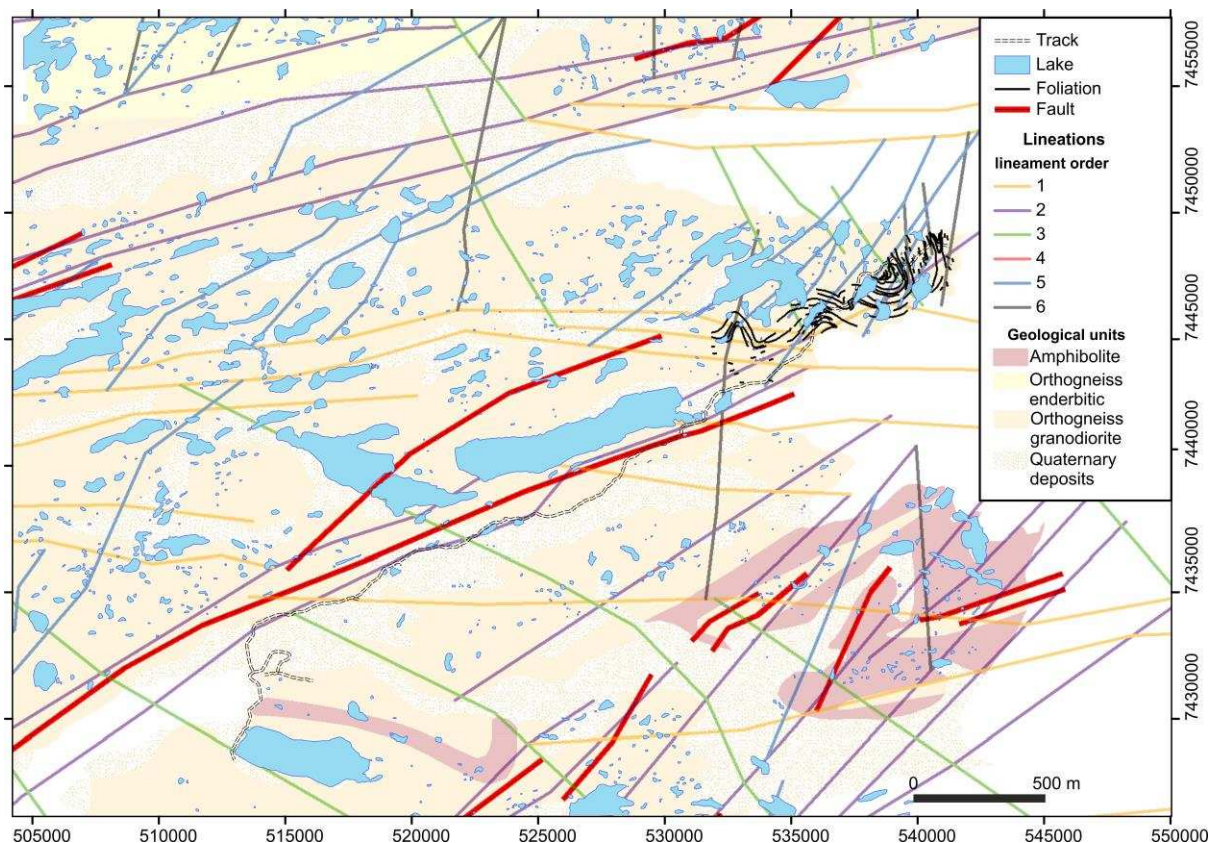
916

917

918

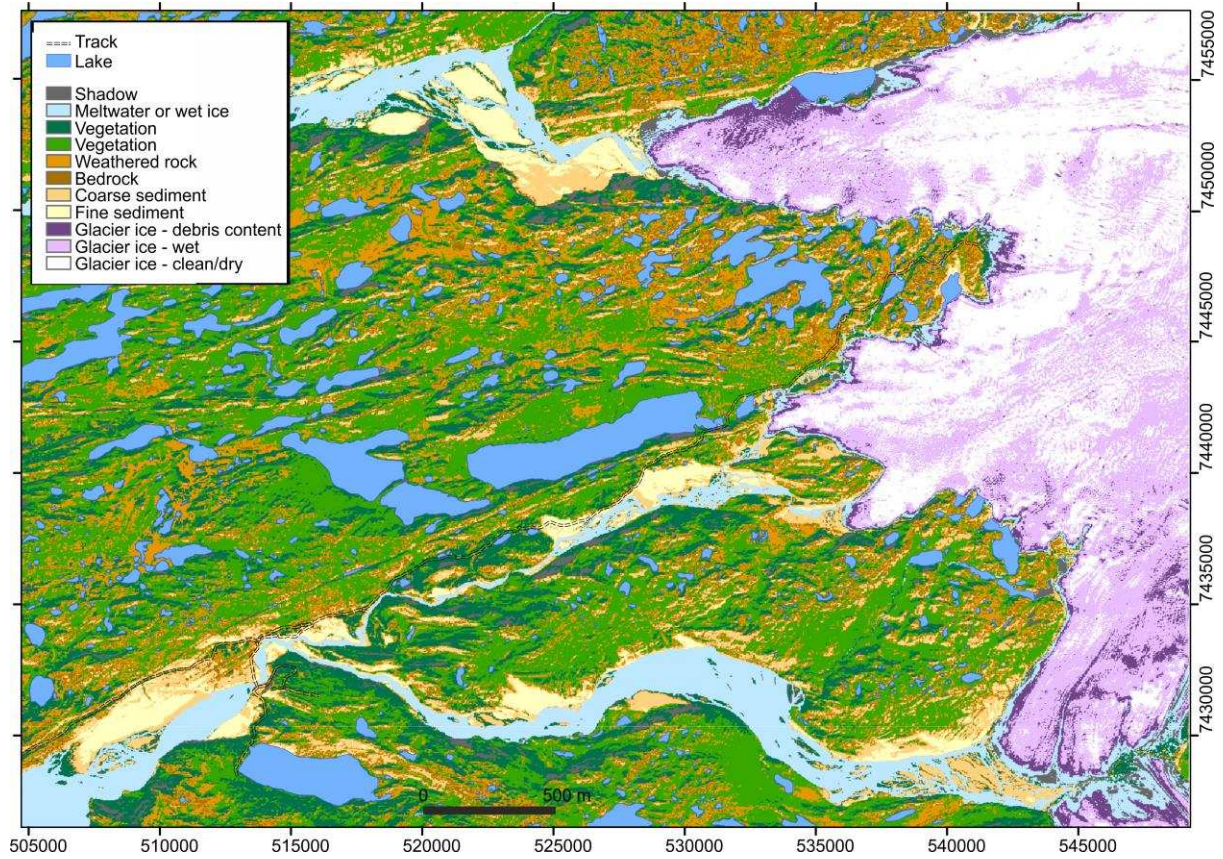
919

920



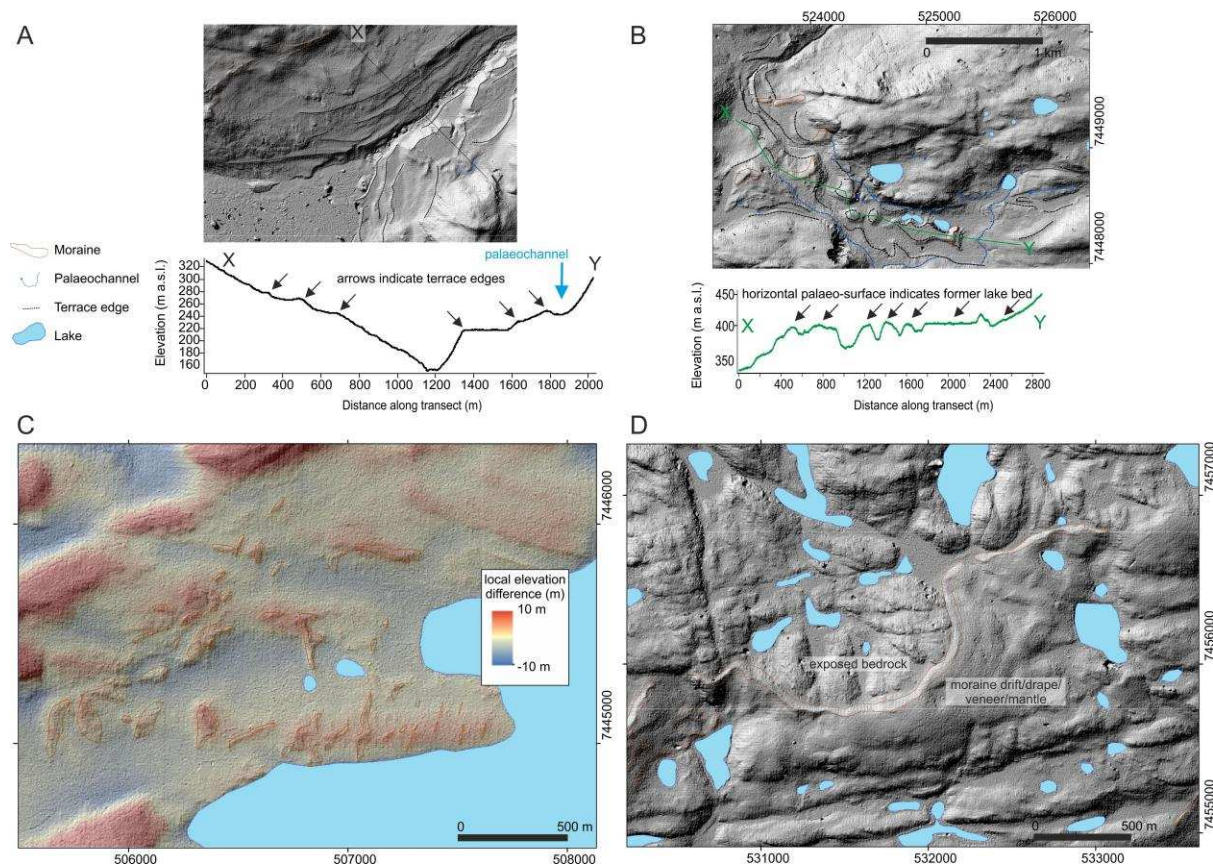
921
922
923
924
925
926
927
928
929

Figure 2. Geology of the Kangerlussuaq – Russell Glacier area adapted from the 1:500 000 mapping of Pedersen *et al.* (2013) and GEUS (2013). Pedersen *et al.* (2013) report that the lineaments are hierarchical and relate to structural features in crystalline rocks such as faults and shear zones, rock fabrics and discontinuities due to differences in rheology or competence.



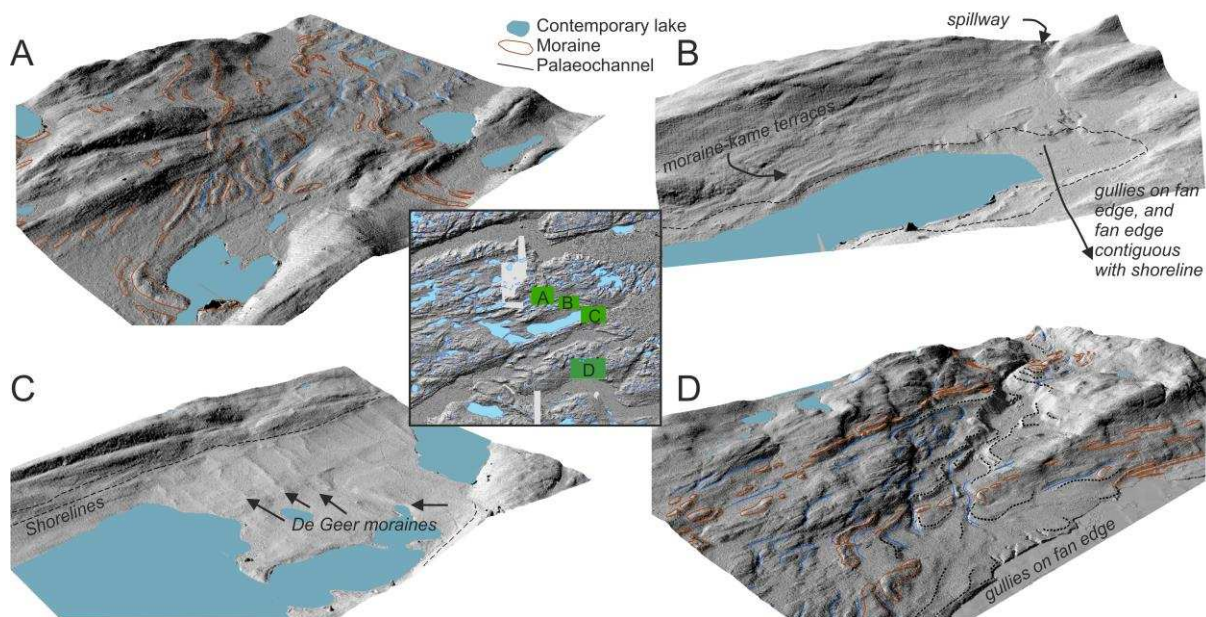
930
931
932
933
934
935
936
937

Figure 3. Landcover classification of the Kangerlussuaq – Russell Glacier area, achieved using 30 m cell size bands 2 - 7 of a Landsat 8 image and an ISODATA clustering algorithm.



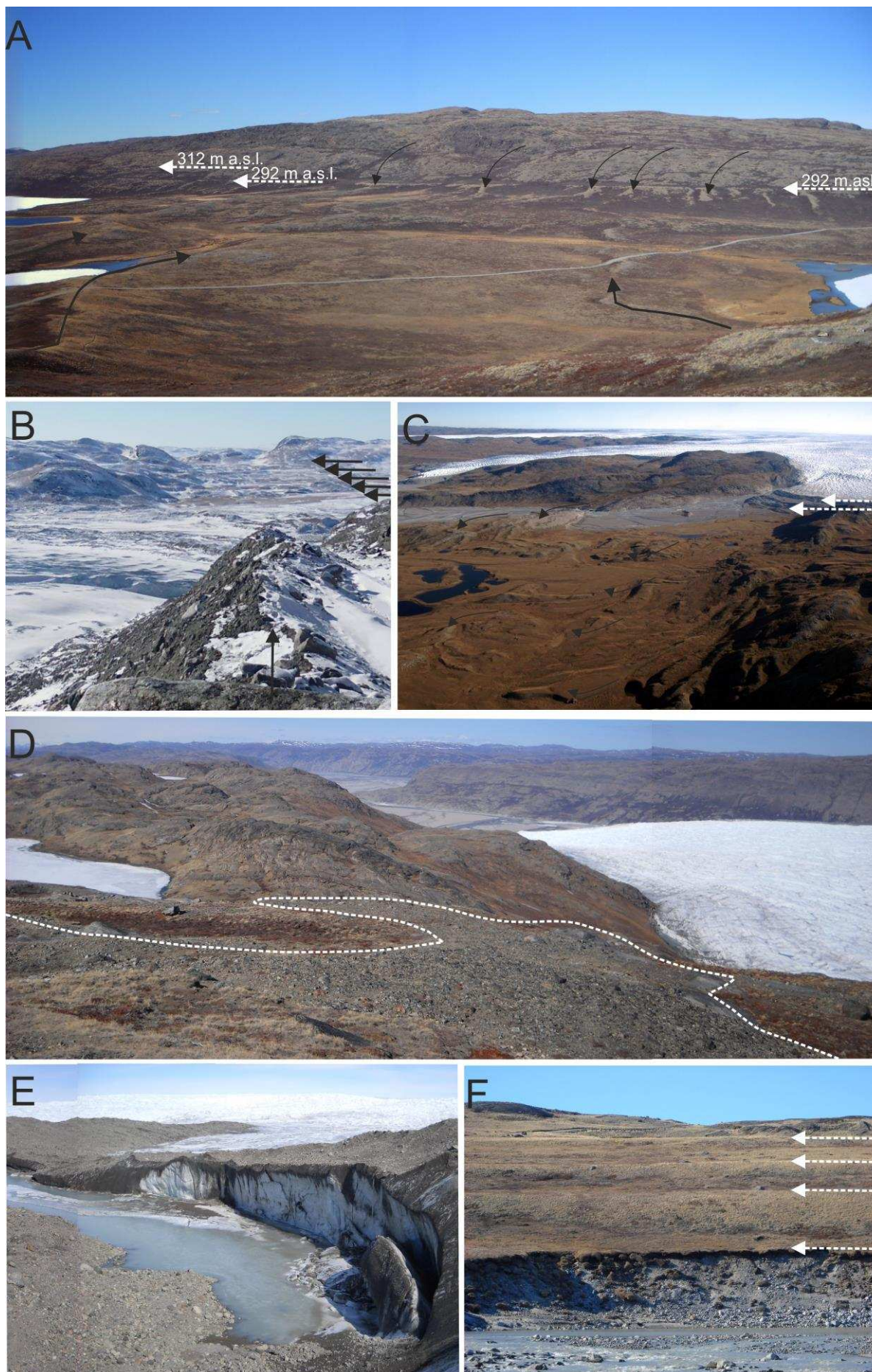
938
939
940
941
942
943
944
945
946
947
948

Figure 4. Examples of digital criteria used to identify glacial landforms, including elevation transects, in this case of asymmetric terrace edges (A), 3D visualisation of palaeochannels and transect of elevation (green line) (B), elevation deviations from a local trend to identify subdued moraine ridges (C), and visual assessment of surface texture to identify moraine drift/veneer/drape deposits (D). The location of these panels is indicated in Fig. 7.



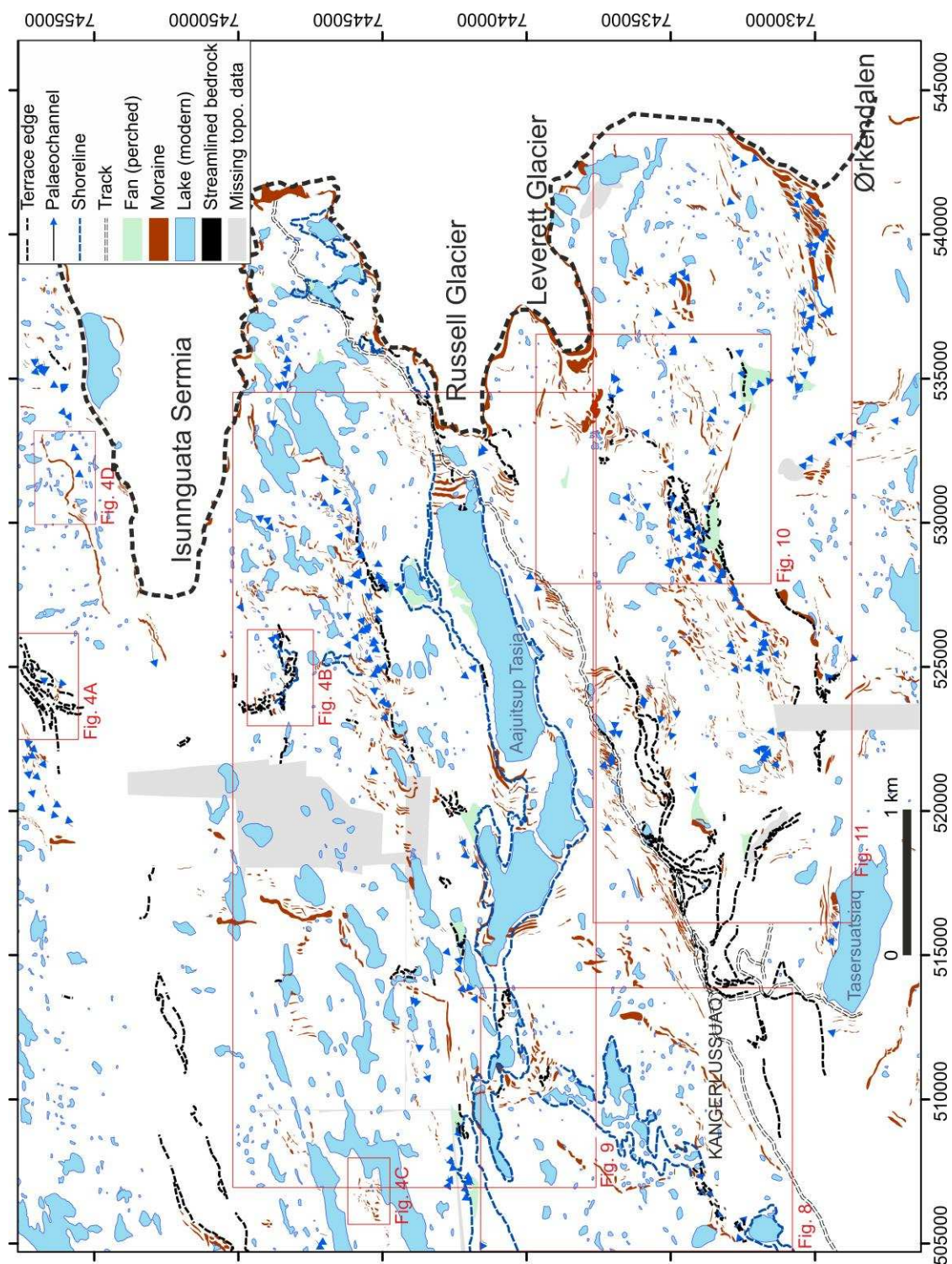
949
950
951
952
953
954
955
956
957
958
959

Figure 5. 3D visualisation of four sub-areas to illustrate landform type, geometry, position and context, specifically: the occurrence and character of major and minor moraine ridges (A), stacked terraces within a bedrock gorge and palaeochannels on hillsides and plateau surfaces (B), shorelines and De Geer moraines (C), and shorelines and perched fan-shaped deposits with incised edges (D). Note moraines and palaeochannels are visible in panels C and D but not encircled to maintain clarity of their topographic signature. Note that scale varies due to perspective of view.



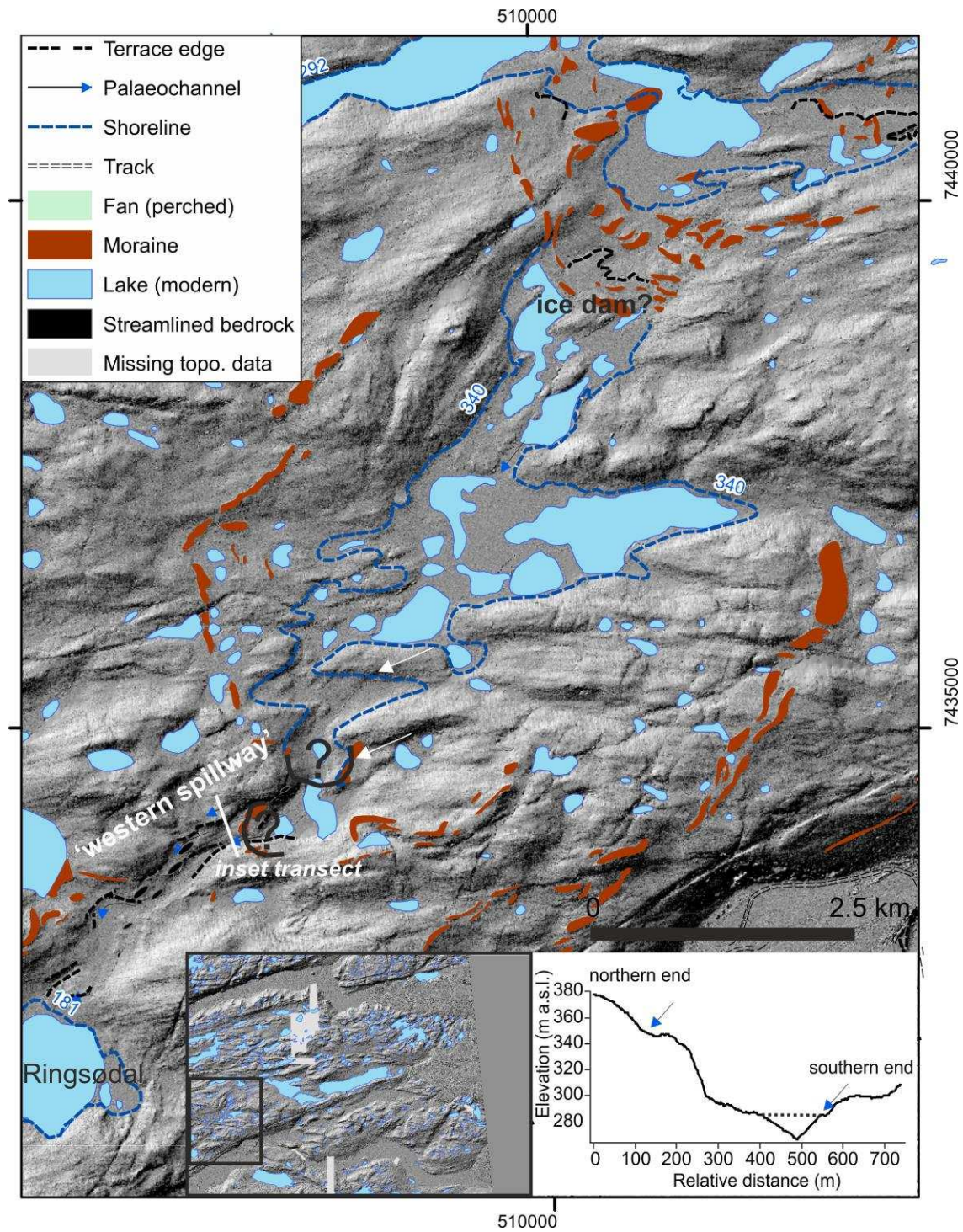
961 **Figure 6.** Field photographs depicting examples of: shorelines (white arrows) and De
962 Geer moraine ridges (black arrows) at easternmost end of Aajuitsup Tasia (A), and
963 contemporary lateral moraine (vertical line) and moraine-kame terrace complex
964 (horizontal arrows) in Leverett Glacier proglacial area (B), push moraine complex
965 (white arrow) and mid-Holocene moraines (black arrows) at Leverett Glacier (C), patch
966 of till/drift mantle/veneer on otherwise scoured bedrock surface immediately south of
967 Isunnguata Sermia (D), stagnating ice with veneer of melt-out sediment at easternmost
968 end of track (E), shorelines immediately adjacent to contemporary river draining
969 northern flank of Russell Glacier (F). Image forming panel B is courtesy of Neil Ross C
970 and image forming panel is courtesy of Andrew Tedstone.

971
972
973
974
975
976
977
978
979
980
981
982
983
984
985
986
987
988
989
990
991
992



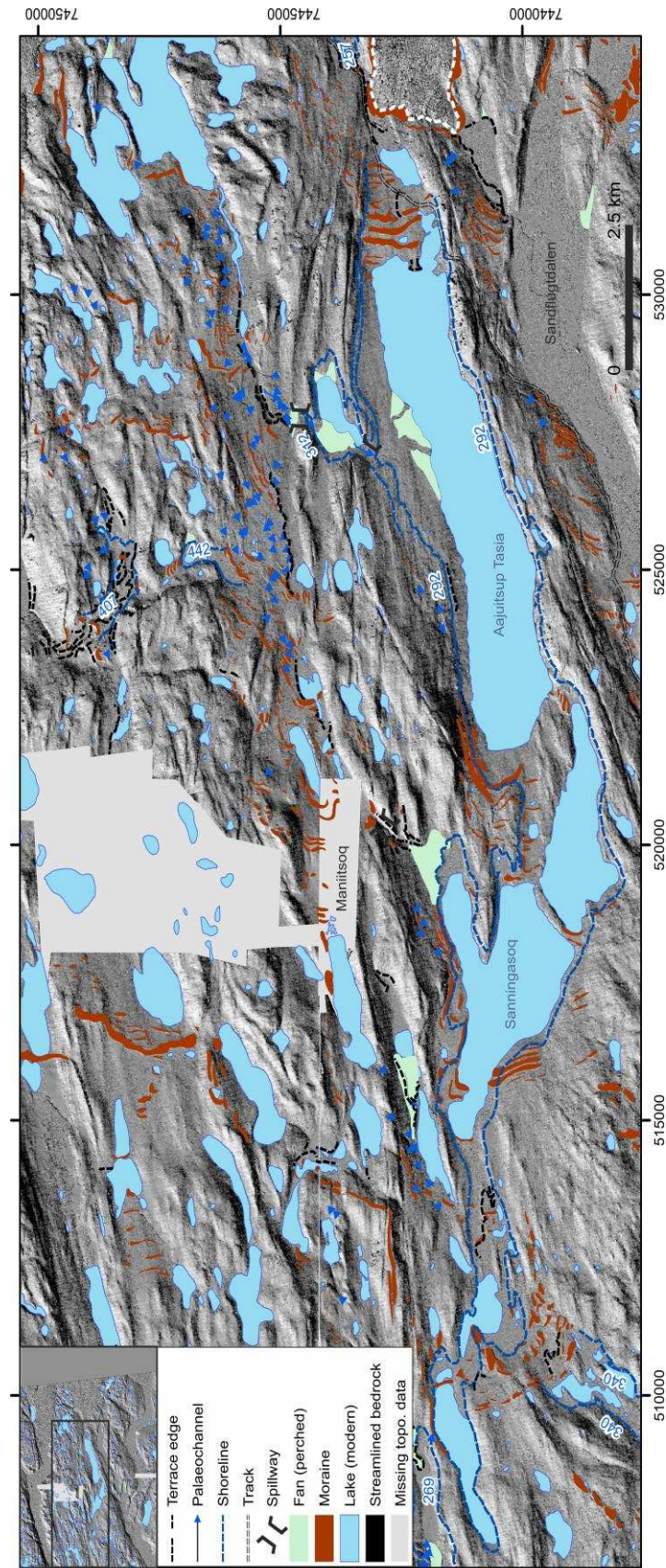
993
 994
 995
 996
 997
 998
 999
 1000
 1001
 1002

Figure 7. Overview of the glacial geomorphology in the Kangerlussuaq – Russell Glacier area. The present day ice margin is represented by black dashed line. A .pdf version of this map (without the other figure location outlines) enabling zoom, panning and with layers that can be switched on and off is available as [Supporting Information \(Fig. S7\)](#).



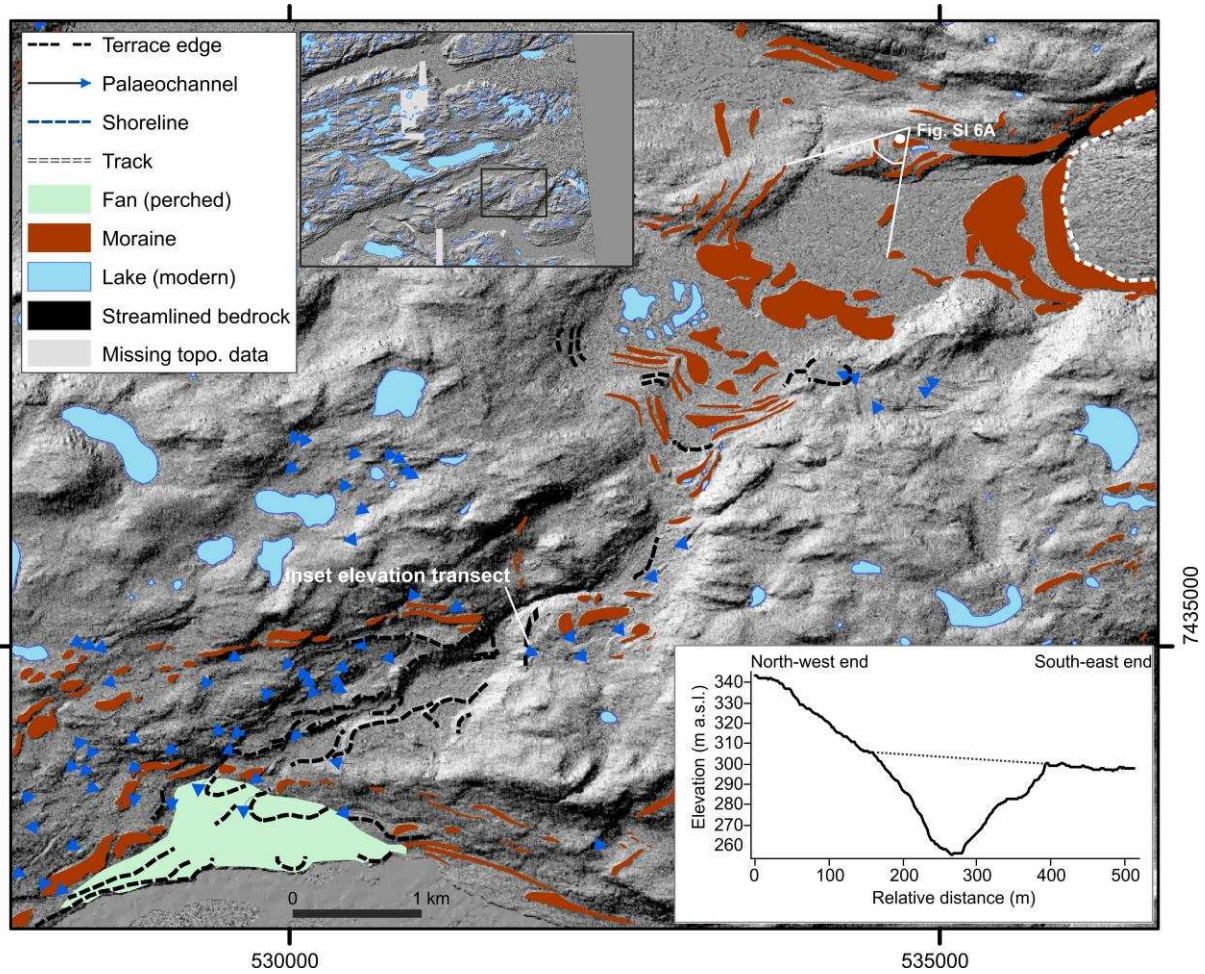
1003
1004
1005

Figure 8. Glacial geomorphology of the western spillway and associated palaeolake.



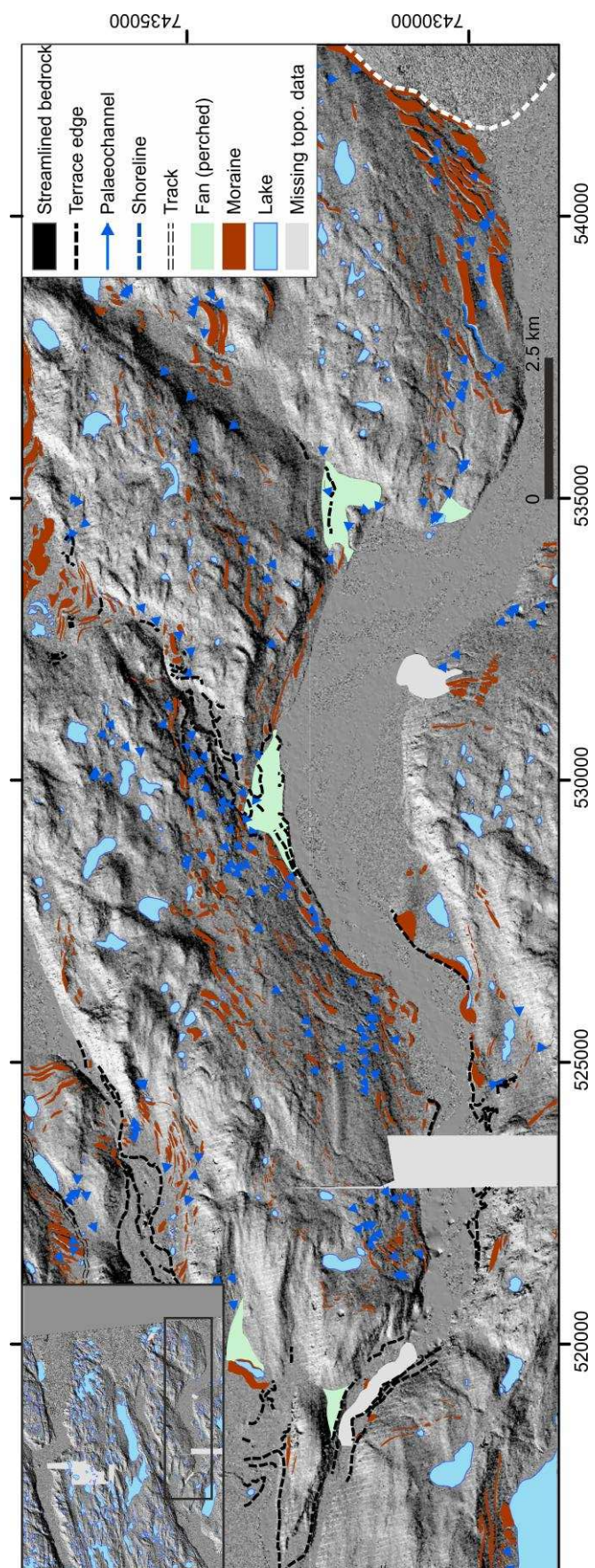
1006
1007
1008
1009
1010

Figure 9. Glacial geomorphology of the Aajutsup Tasia complex, highlighting evidence of shorelines and meltwater routing over several major spillways. The present day ice margin is represented by white dashed line.



1011
1012
1013
1014
1015
1016
1017
1018
1019
1020
1021
1022
1023
1024

Figure 10. Glacial geomorphology of the palaeochannel emanating from the Leverett Glacier proglacial area. The present day ice margin is represented by white dashed line.



1025
1026
1027

Figure 11. The Ørkendalen marginal moraines and meltwater channels. The present day ice margin is represented by white dashed line.

1028

Description	Landform	Interpretation
Discontinuous ridges, often sinuous and hummocky along crest, and extends across landscape, especially in subparallel sets linking those on shallow gradient slopes with those across valley floors	Moraine ridge	Major complexes indicative of ice margin advance and minor ridges indicative of still-stand during recession
Sub-parallel ridges with sub-parallel and curved crests that trend transverse to (palaeo) ice flow and situated altitudinally below palaeolake shoreline	De Geer moraine	Indicative of seasonal advances during grounding line retreat
Discontinuous ridges on valley sides with relative smooth elevation profile along crest and especially with numerous parallel sets	Moraine-kame terrace complex	Indicative of ice marginal meltwater reworking moraine during ice surface lowering
Nested, sinuous and incised channel sets subparallel to topographical contours	Meltwater palaeochannel	Channel formed during ice surface lowering. Possibly subglacial if partly in bedrock
Pitted and hummocky surface, often with oversized boulders	Till/drift mantle/veneer	Subglacial deposition during glacier stagnation and passive ice margin retreat
Near-horizontal surface with smooth texture, often with identifiable bench especially in embayments. Exactly parallel to topographic contours and partially encircling a topographic basin	Shoreline	Former ice- or moraine-dammed lake
Sinuous channel with steep sides and streamlined bedrock hummocks within it, often over a col	Spillway	Major palaeochannel, probably carved during sudden lake outburst flood
Fan-shaped landform comprising gently-sloping top and steep foreslope, situated above modern lake level	Perched delta	Indicative of former sediment-charged fluvial system and of former lake level/base level
Horizontal terrace edges	Incised braidplain or marine terrace	Change in base level and/or meltwater-sediment regime
Sloping terrace edges	Incised fluvial fan or delta	Change in base level and/or meltwater-sediment regime

1029

1030 **Table 1.** Geomorphological criteria to identify ice marginal and subglacial landforms in
 1031 west Greenland, developed in part from Tables 1 and 2 of Perkins & Brennand (2015) and
 1032 in part from the digital topographical analyses of this study.

1033

1034

1035

1036

1037

1038

1039

1040

1041

1042

1043

1044

1045

1046

1047

1048

1049

1050

1051

1052

1053

1054

1055
1056
1057
1058
1059
1060
1061
1062
1063
1064
1065
1066
1067
1068
1069
1070
1071
1072
1073
1074
1075
1076
1077
1078
1079
1080
1081
1082
1083
1084
1085
1086
1087
1088
1089
1090
1091

Supporting Information

Word document containing a description of method used to obtain, process and correct fine-resolution topography, and geology and landcover datasets

All Supporting Information figures are available as separate image files, except figure S 7 which is a .pdf format.

Figure S 1 Dates of imagery used to construct the 2m grid SETSM DEM of the Kangerlussuaq – Russell Glacier area. Colours denote year groups.

Figure S 2A SETSM DEM tiles *before* relative vertical correction

Figure S 2B SETSM DEM tiles *after* relative vertical correction

Figure S 3 Comparison of grid cell elevations of SETSM (2m grid) with airborne laser scanner (ALS) data (2m grid), *before* (A) and *after* (B) horizontal co-registration.

Figure S 4 Comparison of grid cell elevations of SETSM (2m grid) DEM tiles with dGPS 3D points, a 2m ALS DEM, a 5m DEM from traditional photogrammetry, and an ASTER DEM (A). The ASTER DEM and the 5m DEM are apparently uncorrected for the geoid. The western-most SETSM tile was 3.5 m lower than the dGPS and ALS data (B). In contrast the eastern-most SETSM tile had elevations that were in good agreement with the dGPS data, as indicated by the ellipse in panel C.

Figure S 5 Comparison of ALS 2m DEM (A) with the adjusted SETSM 2m DEM (B). Note SETSM DEM is rougher, arguably more noisy, due to interpolation between matched points identified in the SETSM photogrammetry algorithms.

Figure S 6 Field photographs of Leverett forefield (A) and of ice margin between Isunnguata Sermia and Russell Glacier (B).

Figure S 7 Mapped geomorphology overlain on hillshaded DEM, in a .pdf file with zoom and pan functions and with layers (e.g. moraines, palaeochannels) that can be switched on and off.

<please see accompanying .pdf file>

Supporting Information

Datasets and methods

Fine-resolution topography

Topography at high-resolution (2m grid) was downloaded in four tiles to cover the study area from the University of Minnesota Polar Geospatial Center (PGC) website: <http://www.pgc.umn.edu/elevation/stereo>. These digital elevation models (DEMs) were produced by the PGC using photogrammetric processing of stereo-pairs of DigitalGlobe imagery, specifically via the Surface Extraction with Triangulated Network-based Search-space Minimization (SETSM) algorithms (Noh and Howat, 2015). Note that this is a composite DEM, the seamless coverage being constructed from multiple image pairs from multiple flight lines from multiple dates (Fig. S 1).

Readers may wish to note that similar quality of glacial geomorphology mapping can now be achieved elsewhere in west Greenland (and in some other parts of the Alaskan and Canadian arctic) because SETSM DEM production by the PGC is ongoing. As high-resolution topographic data become available for more remote regions, via automated processing such as SETSM, the opportunity to exploit the excellent preservation of landforms within semi-arid arctic, sub-arctic and sub-polar environments will develop further.

We made a three-step evaluation of the 3D quality of the SETSM DEMs. Firstly, all datasets were projected to UTM zone 22N. We then compared elevations of overlaps of the four adjacent SETSM DEM tiles for relative consistency. One tile was found to have grid cell elevation values that were on average 3.44m higher than the other tiles and this was adjusted to best-fit (Fig. S 2). Following the relative vertical shift, the four SETSM DEM tiles were mosaicked and then this mosaic was horizontally adjusted, or 'co-registered' to our ALS data, the horizontal shift applied was -3.61m in the x direction, i.e. westwards, and +4.10m in the y direction, i.e. northwards (Fig. S 3). The vertical and horizontal adjustments made individually and in combination in this study are within the 4.44 Circular Error (CE) reported by Noh and Howat (2015) for the flight strip WV02_20100819 (their Table 2).

Finally, for absolute elevation checks we compared the SETSM mosaic DEM (2m grid) elevations to those of (i) an ASTER DEM (30m grid), (ii) a DEM (5m grid) produced using standard photogrammetry on 1:10,000 scale aerial photographs and as described in Carrivick et al. (2013), (iii) an airborne laser scan (ALS) dataset (gridded at 2m) as obtained from the UK Natural Environment Research Council (NERC) Airborne Research and Survey Facility (ARSF) campaign IPY07-03, and (iv) to ~ 10,000 differential Global Positioning System (dGPS) 3D coordinates as obtained over multiple field seasons and as utilised in Russell et al. (2011) and Carrivick et al. (2013), for example. The spatial coverage of each of these four topographic datasets is given in [Figure 1](#) and notably encompasses wide swaths of land, which is in stark contrast to the NASA Operation IceBridge data, which is predominantly over ice and entirely composed of narrow strips, but nonetheless used by Noh and Howat (2015) for vertical elevation checks of the SETSM DEM. Our (absolute) elevation analysis identified excellent agreement in dGPS-derived elevations and in ALS-derived elevations and thus realised the necessity for a +3 m vertical shift of the SETSM DEM mosaic ([Fig. S 4](#)).

The resultant SETSM mosaic DEM as modified and utilised in this study is of an unprecedented fine-resolution given its spatial extent, but surfaces tend to be rougher, perhaps more noisy, than similar resolution ALS data ([Fig. S 5](#)). This 'roughness' is most likely due to interpolation between matched points that were identified in the SETSM photogrammetry algorithms (Noh and Howat, 2015).

Additionally, 1080 lake polygons were digitised to (i) provide a map layer for ease of navigation/orientation, and (ii) to mask them from the DEM, because although the SETSM algorithm was designed to reconstruct a water surface (Noh and Howat, 2015) we found that across this study site there were big errors in the DEM over and around lakes, probably due to reflectance issues in the optical imagery, shadow, partial snow cover, frozen or partially frozen water and boulders protruding through shallow water surfaces. We could not use the binary raster grids of calculated/interpolated elevation as provided automatically by the SETSM algorithm because at fine-resolution the interpolated grid cells included a lot of land surface other than lakes.

Finally, the SETSM DEM and the associated hillshade image of this DEM were visually inspected for remaining errors, most notably those caused by snow patches. Whilst we erred on the side of retaining as much data as possible particularly bad (massive spikes or sinks) errors were manually removed.

Geology and landcover

Geological unit lithology (Figure 2) was digitised as polygons from that mapped at 1:500,000 (Pedersen et al., 2013; GEUS, 2013). Major faults, regional lineations and local foliation (Figure 2) were digitised as polylines from that mapped by Klint et al. (2013). Due to the relatively coarse scale of the original mapping, both the geological polygons and the geological polylines were manually adjusted (by eye) to best-fit the position of the same features evident in the high-resolution topography.

Landcover (Figure 3) was classified using an ISODATA clustering algorithm applied to a Landsat 8 (operational Land Imager) scene acquired on 12th July 2014. Bands 2 – 7 (all 30 m spatial resolution) were used and the required number of classes was set at fifteen. This number of classes provided the optimum balance between class separation and class redundancy. The classification was subsequently validated in the field, primarily along a 30 km transect in the vicinity of the vehicle track (Figure 3). Dry southern slopes and plateau are dominated by steppe vegetation, specifically grasses and sedges (e.g. *Carex supina*, *Kobresia myosuriodes*, *Poa glauca*, *Calamagrostis purpurascens*, *C. poluninii* and *Salix glauca*). Wetter northern slopes and hollows were dominated by slightly taller vegetation (e.g. *Betula nana*, *Carex norvegia*, *Juncus arcticus* and *Rhododendron tomentosum* or 'Ledum palustre'). Aeolian sediments often appeared to be overgrown with *Calamagrostis purpurascens*, *Artemisia borealis* and *Rumex acetosella* (Génsbøl, 2004; Willemsse 2003). Some manual editing of the landcover was necessary because some snow patches, which we identified with comparisons to optical imagery and to the high resolution topography, were misclassified as water. The final landcover classification (raster image) was adjusted in horizontal position by -26.00 m in the X direction (i.e. west) and by +18.3 m in the Y direction (i.e. north) to best-fit our high-resolution topography.

Figure S 2A

SETSM DEM tiles *before* relative vertical correction

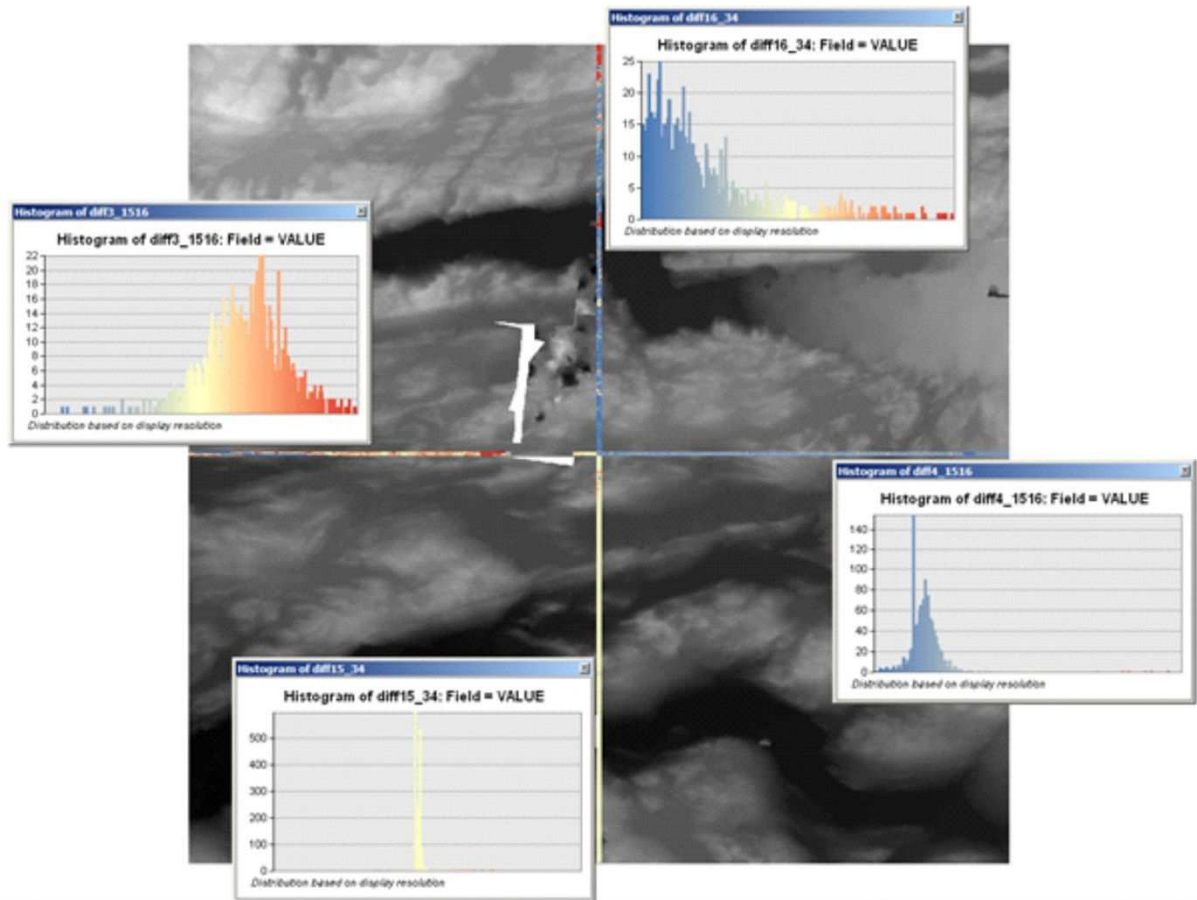


Figure S 2A

SETSM DEM tiles *before* relative vertical correction

Figure S 2B

SETSM DEM tiles *after* relative vertical correction

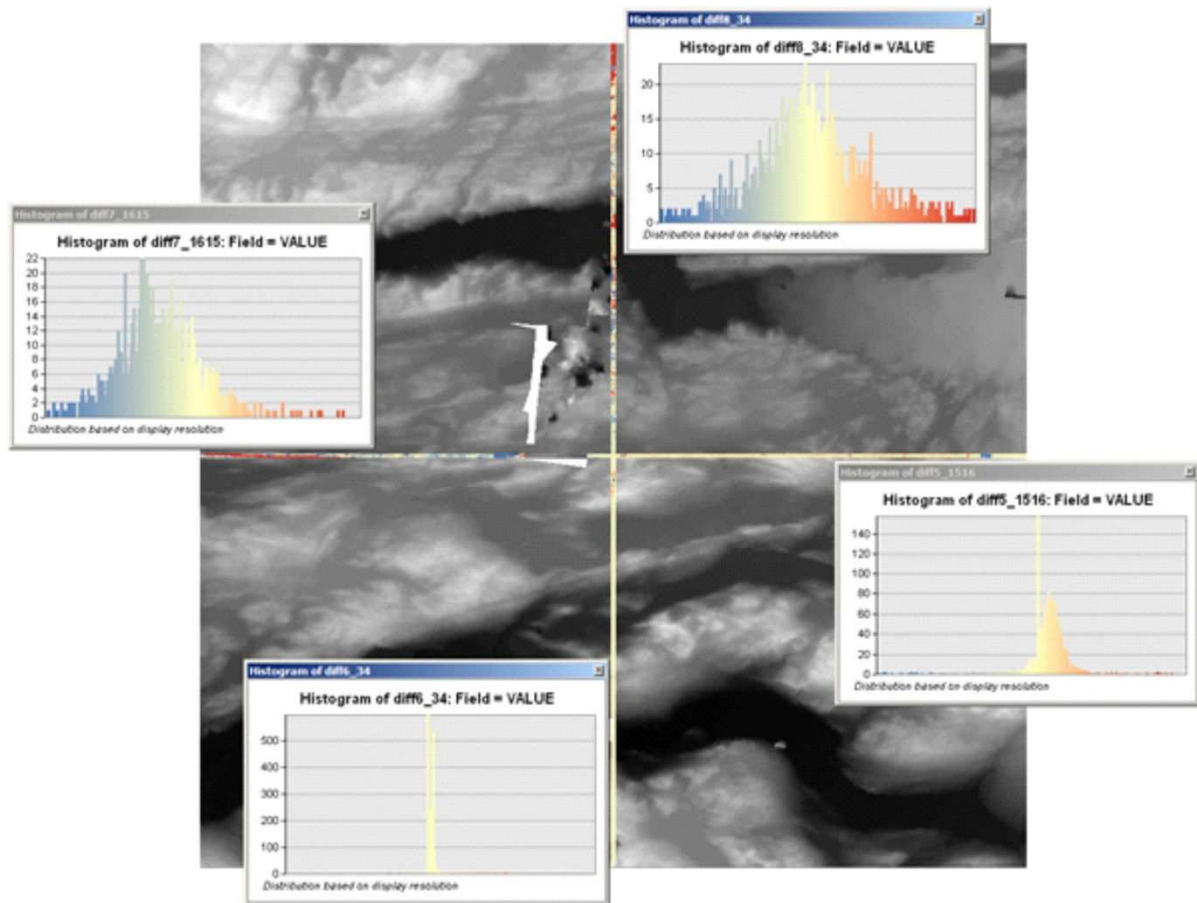


Figure S 2B

SETSM DEM tiles *after* relative vertical correction

Figure S 3

Comparison of grid cell elevations of SETSM (2m grid) with airborne laser scanner (ALS) data (2m grid), *before* (A) and *after* (B) horizontal co-registration.

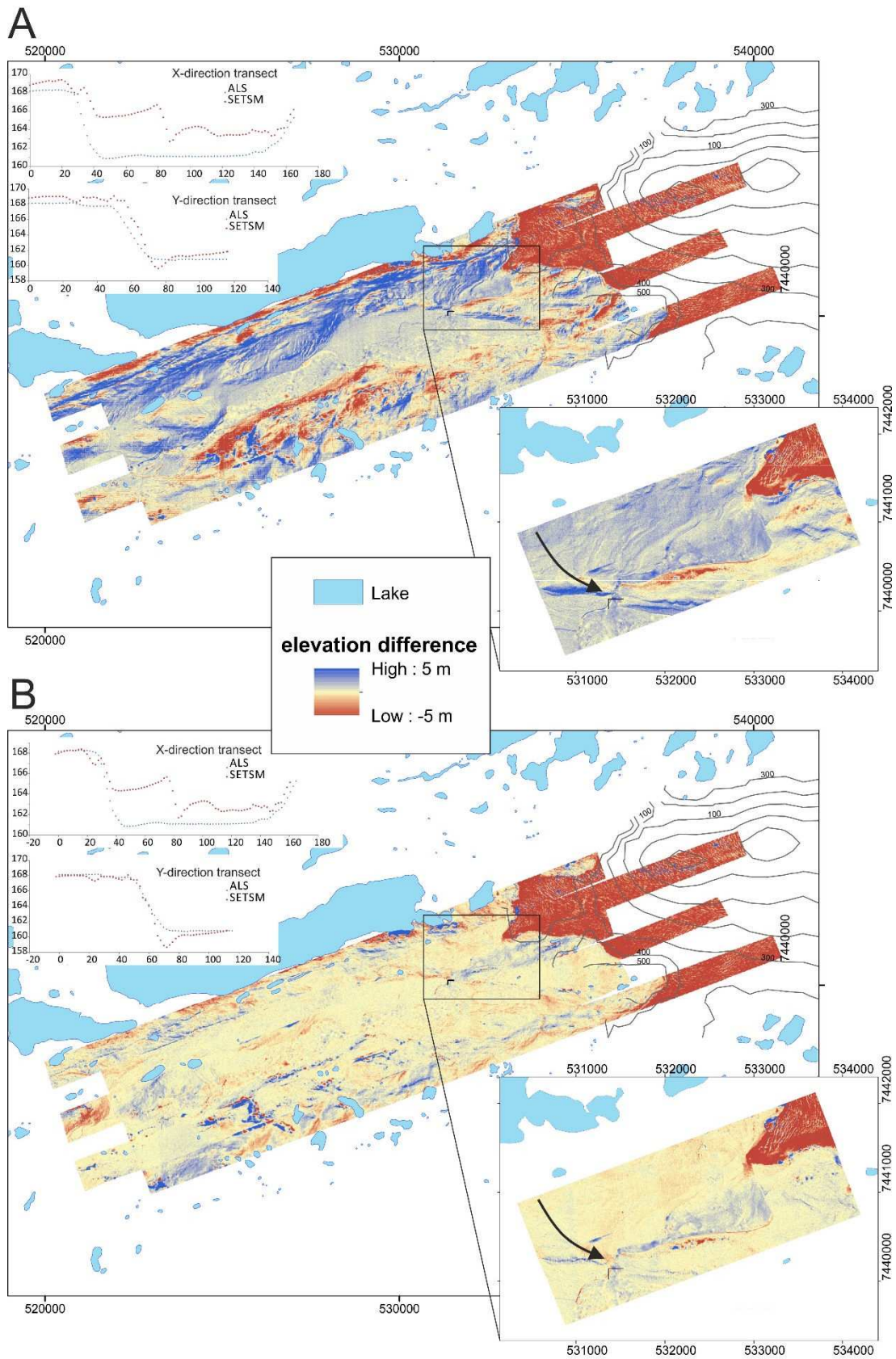


Figure S 3

Comparison of grid cell elevations of SETSM (2m grid) with airborne laser scanner (ALS) data (2m grid), *before* (A) and *after* (B) horizontal co-registration.

Figure S 4

Comparison of grid cell elevations of SETSM (2m grid) DEM tiles with dGPS 3D points, a 2m ALS DEM, a 5m DEM from traditional photogrammetry, and an ASTER DEM (A). The ASTER DEM and the 5m DEM are apparently uncorrected for the geoid. The western-most SETSM tile was 3.5 m lower than the dGPS and ALS data (B). In contrast the eastern-most SETSM tile had elevations that were in good agreement with the dGPS data, as indicated by the ellipse in panel C.

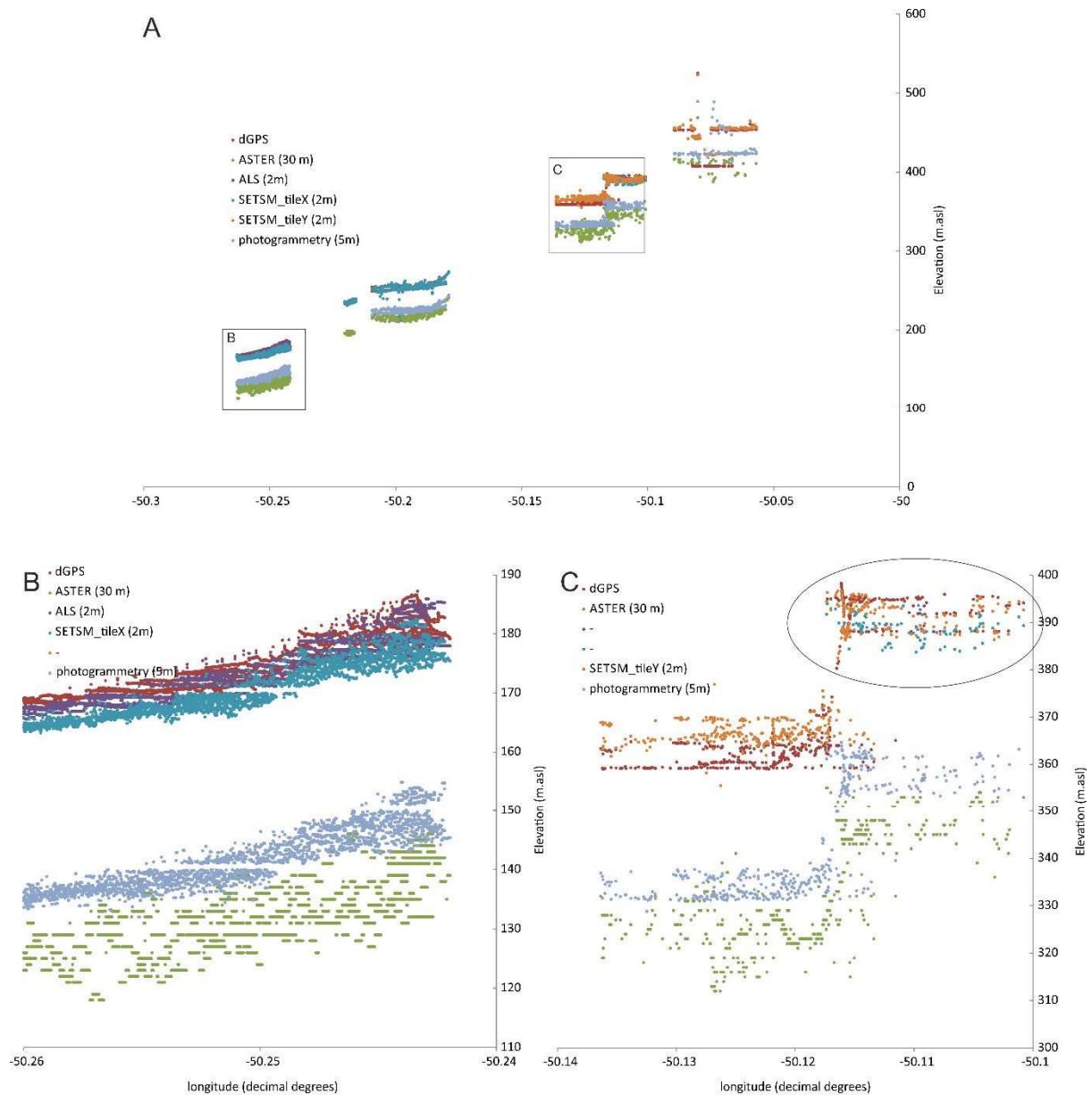


Figure S 4

Comparison of grid cell elevations of SETSM (2m grid) DEM tiles with dGPS 3D points, a 2m ALS DEM, a 5m DEM from traditional photogrammetry, and an ASTER DEM (A). The ASTER DEM and the 5m DEM are apparently uncorrected for the geoid. The western-most SETSM tile was 3.5 m lower than the dGPS and ALS data (B). In contrast the eastern-most SETSM tile had elevations that were in good agreement with the dGPS data, as indicated by the ellipse in panel C.

Figure S 5

Comparison of ALS 2m DEM (A) with the adjusted SETSM 2m DEM (B). Note SETSM DEM is rougher, arguably more noisy, due to interpolation between matched points identified in the SETSM photogrammetry algorithms.

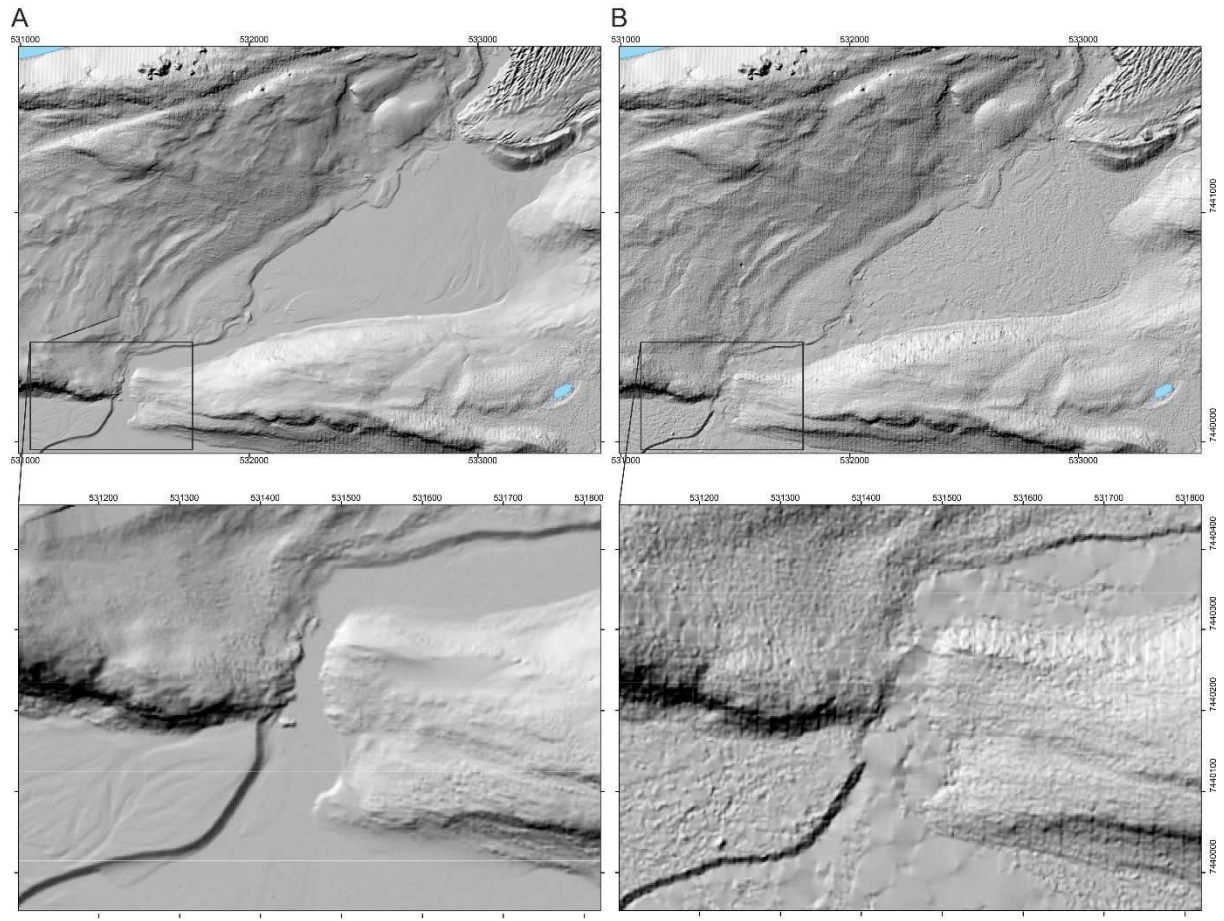


Figure S 5

Comparison of ALS 2m DEM (A) with the adjusted SETSM 2m DEM (B). Note SETSM DEM is rougher, arguably more noisy, due to interpolation between matched points identified in the SETSM photogrammetry algorithms.

Figure S 6

Field photographs of Leverett forefield (A) and of ice margin between Isunnguata Sermia and Russell Glacier (B).



Figure S 6

Field photographs of Leverett forefield (A) and of ice margin between Isunnguata Sermia and Russell Glacier (B).

Figure S 7

Mapped geomorphology overlain on hillshaded DEM, in a .pdf file with zoom and pan functions and with layers (e.g. moraines, palaeochannels) that can be switched on and off.

<please see accompanying .pdf file>

